Title
Vesicular monoamine transporter trafficking affects mode of neurotransmitter release and microcircuit function

Author
Asuncion, James Edward Laurel Dizon

Publication Date
2020

UNIVERISTY OF CALIFORNIA

Los Angeles

Vesicular monoamine transporter trafficking affects mode of neurotransmitter release and microcircuit function

A dissertation submitted in satisfaction of the requirements for the degree of

Doctor of Philosophy in Neuroscience

by

James Edward Laurel Dizon Asuncion

2020

ABSTRACT OF THE DISSERTATION

Vesicular monoamine transporter trafficking

affects mode of neurotransmitter release and microcircuit function

by

James Edward Laurel Dizon Asuncion

Doctor of Philosophy in Neuroscience

University of California, Los Angeles, 2020

Professor David E Krantz, Chair

Monoamine neurotransmitters, such as dopamine and serotonin, modulate fast synaptic transmission in circuits that mediate many complex behaviors including aggression, sleep, attention, and mood. In psychiatry, many therapeutics target monoamine systems at either the receptors or transporters that mediate and regulate monoamine neurotransmission. The vesicular monoamine transporter (VMAT) is responsible for loading all monoamine neurotransmitters into both synaptic vesicles (SVs) and large dense-core vesicles (LDCVs), which mediate synaptic and extrasynaptic release, respectively. However, the functional contribution of each type of vesicular release to circuit function and behavior is unknown. Previous studies in *Drosophila* have demonstrated that the amount and site of amine release can be altered by mutations in the C-terminal trafficking domain of *Drosophila* VMAT (DVMAT). In a *DVMAT- null* genetic background, the function of several circuits and behaviors are perturbed, but are rescued by transgenic

expression of wild-type and trafficking mutant alleles. Some behaviors are not rescued by trafficking mutants. Mutations that cause DVMAT to preferentially traffic to LDCVs do not rescue fertility and egg-laying deficits. This suggests that the oviposition circuit is highly sensitive to the delicate balance between synaptic and extrasynaptic release of the neurotransmitter octopamine. I hypothesized that trafficking mutations in the endogenous *DVMAT* gene locus confer circuit dysfunction, resembling genetic rescue experiments. To further test this idea, I created a new genetic model of DVMAT trafficking using CRISPR/Cas9 to alter trafficking signals in the endogenous gene. This novel genetic model will be useful to study the effects of mutants at endogenous expression levels, facilitates combinations with genetic and molecular tools for circuit analysis, and represents a new platform for genetic screens to find novel regulators of DVMAT function. The work presented here investigated the contributions of the different modes of monoamine release and the neuroanatomy of the model circuit. I found that mutations in VMAT trafficking caused a decrease in response from the post-synaptic target organ. These and further studies elucidate novel mechanisms of aminergic signaling and new avenues for the research and development of new therapeutics for psychiatric disorders.

The dissertation of James Edward Laurel Dizon Asuncion is approved.

Carlos Portera-Cailliau

Felix Erich Schweizer

Jeffrey Michael Donlea

Stephen Lawrence Zipurksy

David E Krantz, Committee Chair

University of California, Los Angeles

2020

Dedication

For Zazu and Marley

For Annie and Andrew

For Dad, who I miss every day.

For my family

For Mom

For Anna, who keep me going each day.

Table of Contents

List of Figures, Tables, Supplementary Materials

Figures

Appendix

Media uploads

Wild-type and DVMATΔ3 optogenetic experiments

AVI video files:

WT example 20200310.avi

DVMATD3 example 320200228.avi

TDC2 Multi-Color Flp-Out – example images

TIFF image file: MCFO matrix.tif

Acknowledgements

First I want to thank David Krantz, the principal investigator. Thank you for your support and mentorship over the years and helping me develop into a physician-scientist.

Aditya Eamani worked with me on the work in chapters 1 and 4. She taught me the foundations of working in the lab, on *Drosophila*, and how to accomplish experimental goals. I thank her for allowing me to share our data here.

Sonali Deshpande worked with me on the work in chapters 2 and 3. She taught me the importance of rigor and a critical eye, and how to be a diligent and precise experimentalist.

Ethan Rohrbach worked with me on the work in chapter 2. Without his help, I would have struggled to complete the work and have publishable images. I thank him for allow me to share his data here.

Daniel Suto worked with me on the work in chapter 2 and 4. He was an exceptionally bright undergraduate who taught me the basics of working with *Drosophila* and made significant contributions to start many projects in the lab.

I also thank my fellow scientists in the lab Jenna Harrigan, Kathy Myers, Maureen Sampson,

and Shivan Bonnano. I appreciate their help, feedback, and insights that aided me in developing this work.

I also thank the current and former undergraduates Pranathi Rao, Melissa Trieu, Ellery Schlingmann, Pauline Tze, Rebecca Arnold, Nikoo Dalili, Binu Kandagedon, and Kenneth Li. I appreciate their help and questions that made me think deeply about the work.

I especially thank the administrative support I have had over the years from Susie Esquivel, Josie Alviar, Jenny Lee, Polly Segal, and Ana Elias, without whom none of this is possible. I appreciate their help in keeping me afloat.

I also thank my committee of David Krantz, Carlos Portera-Cailliau, Jeff Donlea, Felix Schweizer, and Larry Zipursky. Their guidance has been crucial for my development as a physician-scientist.

Funding and Support

Thank you to the Medical Scientist Training Program at the David Geffen School of Medicine at UCLA (MSTP NIGMS 5T32GM008042), the Translational Neuroscience of Drug Abuse training program (TNDA NIDA 4T32DA024635) and the National Institute of Mental Health (NRSA 1F30MH115609, R01MH107390) for their financial support of this research and my training.

Vita

I am a medical student in the Medical Scientist Training Program at the UCLA David Geffen School of Medicine since 2013. I received my Bachelors of Arts in Molecular & Cell Biology with emphasis in Neurobiology from the University of California, Berkeley in 2012.

A major influence of my interest in medicine and neuroscience came from having a father who was a general surgeon. I was privileged to receive early exposure to medical and scientific concepts and knowledge that few children ever learn. My late father, Juan Asuncion Jr., M.D., cultivated my curiosity in physiology and medicine from nearly every aspect of our relationship, using it as a teachable moment. In my early childhood, my father's health deteriorated. Yet he used his own illness to teach me about human physiology, pathology, and the standards of care. His life, work, sickness, and death were major driving forces for me to pursue medicine and science. I knew from an early age that I was drawn to medicine like my father. It was a crux where his passion for science met his calling to help others.

My father passed away during my sophomore year at Berkeley. While studying neurobiology, I experienced mental illness. My studies focused on how the brain and mind are intertwined. I was captivated by the intricacies of neurochemistry, especially as it related to substance use, therapeutics, and psychiatry. During that time, my studies and community service activities in Berkeley gave me a platform to contextualize and understand my own illness.

I held a work-study job for 2 years as a laboratory assistant at the Lawrence Berkeley National Laboratory. In my senior year, I received the Rose Hills Foundation Science & Engineering Scholarship which allowed me to leave my work-study job and pursue a richer research experience. I joined the laboratory of HHMI scientist Yang Dan, Ph.D., studying the function of cortical circuits and neuromodulation in mammalian models. I worked with then-post-doctoral fellow Alex Kwan, Ph.D. (now faculty at Yale) to investigate top-down control of visual attention in

the mouse cortex. I was 1 of 4 students from the neurobiology division chosen to present to faculty at the Molecular & Cell Biology Honors Symposium and received the I.L. Chaikoff Award for undergraduate research. I also received honors with high distinction and admission to Phi Beta Kappa.

After graduating from Berkeley, I worked full-time as a technician and teaching assistant at Pomona College. In the laboratory of Jonathan Matsui Ph.D., I worked on and completed ongoing studies in ototoxicity using zebrafish as a model.

Since 2013, I have been enrolled in the David Geffen School of Medicine and its Medical Scientist Training Program. In the last 8 years, I have completed the pre-clinical curriculum, Step 1 of medical licensing, and this current doctoral work in Neuroscience.

My training and research has been supported by National Institutes of Drug Abuse (Translational Neuroscience of Drug Abuse training grant), National Institute of Mental Health (NRSA F30 fellowship), and National institute of General Medical Sciences (Medical Scientist Training Program at UCLA).

Introduction

Aminergic neuromodulation is intimately involved in complex behaviors and psychiatric diseases. Although aminergic drugs are a cornerstone of psychiatric therapy, their mechanisms of action are unknown. In order to better understand the effects of aminergic drugs, neuromodulation, and psychiatric diseases, the molecular biological basis of aminergic signaling must be investigated. This includes understanding the functional relevance of the different modes of neurotransmitter release. Monoamines are released from both synaptic vesicles (SVs) and large dense-core vesicles (LDCVs). SVs contain classic small neurotransmitters, cluster at active zones, and mediate rapid release into the synaptic cleft. LDCVs differ from SVs in that they contain both neuropeptide and classical neurotransmitters and mediate release at extra-synaptic sites. In mammalian neurons, the vesicular monoamine transporter (VMAT2) subcellular localization defines the sites of monoamine storage and has been implicated in modulation of monoamine neurotransmission and pathogenesis of neuropsychiatric disease [1]. In mammalian midbrain dopaminergic neurons, VMAT2 is responsible for loading monoamines into both SVs and LDCVs [1]. It is also known that VMAT2 localizes to vesicles that mediate activity-dependent somatodendritic release of retrograde signals involved in synaptic function, growth, and plasticity. In axon terminals, VMAT2 is localized to LDCVs at sites distant from synaptic active zones [2]. The function and delicate balance of the two release modes, SVs versus LDCVs, have not been experimentally examined in any circuit or behavior.

My dissertation work is significant because I directly addressed this fundamental question. I have studied the effects of monoamine storage and release from different vesicle types by manipulating the localization of the VMAT in *Drosophila* melanogaster (DVMAT). In both mammals and invertebrates, VMATs are responsible for transporting all monoamine transmitters into the lumen of secretory vesicles. Previous studies from David Krantz's laboratory demonstrated that mutations in the trafficking domain are capable of shifting the distribution of DVMAT between SVs

and LDCVs [3, 4]. Signals contained within the DVMAT primary structure, evolutionarily-conserved dileucine- and tyrosine-based motifs, regulate sorting to SVs and LDCVs [4]. Ablation of both of these signals by truncation (Δ3 mutation) or point mutation of the tyrosine-based motif (Y600A) cause redistribution of DVMAT [3, 4]. Wild-type DVMAT sorts about equally to SVs and LDCVs, whereas trafficking mutants preferentially sort to LDCVs.

In DVMAT loss-of-function experiments, loss of monoamine release resulted in dysfunction in a variety of circuits and behaviors [5]. Many of these phenotypes can be rescued by transgenic expression of *DVMAT* wild-type or trafficking mutants [4]. However, some phenotypes, such as infertility due to egg-retention, are not rescued by *DVMAT* trafficking mutant alleles. This suggests that some circuits and behaviors, including the oviposition (egg-laying) circuit, are sensitive to the delicate balance of monoamine release from both SVs and LDCVs. My research aims to uncover underlying mechanisms by which *DVMAT* trafficking mutations cause infertility and defects in oviposition circuit function. Moreover, this is the first study of the different modes of monoamine release, from SVs versus LDCVs, and their differential modulation of downstream targets.

To address these questions, I created a novel trafficking mutant using CRISPR/Cas9 gene editing technology. Simultaneously, I conducted anatomical mapping and functional characterization of octopamine (OA) signaling in the female reproductive tract. Mapping of octopaminergic neurons (OA neurons) to their target organs gives a greater understanding of innervation patterns and potentially regulation of each organ. Similarly, mapping of the different OA receptors can help explain the diverse effects of OA.

These two lines of work allowed me to investigate OA signaling in a model circuit, from both pre- and post-synaptic perspectives. Characterization of OA function the female reproductive system is essential in order understand monoamine release mechanisms. I have since combined these

two lines of work to directly test how the trafficking mutation affects OA function in our model system.

Key Points

Hypothesis: *DVMAT* trafficking mutation Δ3 causes a loss of function in ovulation, with particular focus on lateral oviduct contractions.

Results: In *DVMAT* trafficking mutants in which it is redistributed to primarily to LDCVs and away from SVs, optogenetic stimulation is sufficient to drive contractions, albeit less robust compared to wild-type.

While conducting experiments for *Δ3*, I simultaneously investigated the OA neurons responsible for innervating the female reproductive tract. I found that these neurons innervated the female reproductive system in a segmental and organ specific way.

I also characterized OA's actions on the oviduct, examining the duality of contraction and relaxation.

Together, I demonstrated that OA neurons have highly detailed patterns of innervation that likely accomplish multiple functions of ovulation. I also showed alterations of OA release from primarily LDCVs affects the input onto the oviduct by OA neurons.

These findings pave the way for future investigation into alterations in circuit activity and downstream effects on the reproductive tract. The work presented here is the foundation of future investigation of OA neurons and DVMAT trafficking in the *Drosophila* female reproductive system.

Chapter 1

***DVMAT∆3* CRISPR/Cas9 mutagenesis**

Key Points

Hypothesis: Mutations in the DVMAT C-terminal trafficking domain in the endogenous gene will cause infertility.

Results: I created a novel *DVMAT∆3* mutant that recapitulates previous genetic-rescue experiments.

Creating a new genetic background was crucial to developing new neurocircuitry experiments. Previous work demonstrated the inability of *DVMAT* trafficking mutants to rescue particular phenotypes. While these experiments demonstrated that trafficking mutants cannot rescue certain behaviors, they do not address what specific changes in neural circuit activity is causing the phenotypes.

Genetic rescue experiments have limitations that prevent further investigation into mutant effects on function and activity.

Complicated genetics. Null-mutation genetic background rescued by GAL4/UAS expression of wild-type or mutant alleles. Other expression systems such as LexA/LexAop and QF/QUAS would need to be added for transgenes for experimentation. These systems have much fewer transgenes available in the community. *Drosophila* have 4 chromosome pairs, 3 of which are commonly used for genetic reagents. The many transgenes must be recombined in a way that all of them fit within the 6 chromosomes. This may not be possible because of proximity of transgene and gene loci and decreased viability with each additional transgene.

Expression. The level of expression of rescue alleles is determined by the strength of GAL4/UAS system. These systems will definitely overexpress compared to endogenous gene expression. With the new mutant I created, experiments are improved by

- Mutation of the endogenous gene, preserving endogenous regulation of expression levels
- GAL4/UAS system available for transgenes related to neuroscientific investigation
- Can be further combined with LexA/LexAop system

For these experiments, recombination with *TDC2-GAL4* and *TDC2-LEXA* drivers and various reporter lines can be used to examine how OA signaling is altered by DVMAT-trafficking mutation. With everything combined, I have created genotypes that have the ∆3 mutation, and I can stimulate OA neurons and read activity from OA receptor expressing cells.

Materials and Methods

With CRISPR/Cas9, I mutated the C-terminal trafficking domain of DVMAT. Truncation of the dileucine- and tyrosine-based motifs was accomplished by precise placement of a stop codon upstream of the trafficking motifs, recapitulating the Δ3 mutation (Figure 1B).

Naturally a form of bacterial immunity against viruses, CRISPR/Cas9 has been adapted and widely used for genomic editing [6]. Cas9 is a nuclease that can be guided by RNA to a given sequence of DNA and cleaves it into double strand breaks (DSB). This then triggers either homology-directed repair or non-homologous end-joining. HDR is utilized to incorporate intended mutations into the genome. NHEJ is used to introduce indel mutations.

I designed multiple guide-RNA sequences to target the last coding exon (Figure 1A, 1B) for Cas9-mediated DNA double-strand breakage (DSB). The mutation was introduced during homology-directed repair (HDR) with a single-stranded oligodeoxynucleotide (ssODN) 90-nt long that contained homology arms, the new stop codon, and additional mutations to prevent re-cleavage by Cas9 and to create a restriction digest site (Figure 1B).

The guide RNA is supplied by expression the pU6 expression plasmid [6]. Short ssODNs for the sequence were reverse-complemented and annealed at room temperature. This was the ligated and cloned in the pU6-BbsI-chiRNA expression vector [6], which expresses a guide RNA molecule that consists of the target sequence and PAM and the scaffold to bind to Cas9. This protein-RNA complex has nuclease activity directed by the target sequence and cleaves 3 nucleotides 5' to the PAM.

Exogenous DNA that contains our desired sequence to serve as the repair template. The DNA is supplied in molar excess by either a single-stranded oligodeoxynucleotide (ssODN) or by a double-stranded plasmid. The ssODN must be the sense strand for repair to occur in the correct direction. Mutating the PAM ensures that the ssODN will be intact when supplied to the Cas-9 expressing cells.

Vas-Cas9 flies express Cas9 in only germline cells and were injected with a plasmid encoding the guide RNA and the ssODN to create germline mosaics. Multiple genetic crosses were done to generate stable fly lines. Each line was screened by PCR and restriction digest to probe for the intended stop codon and restriction site.

DNA was then separated by agarose gel electrophoresis (Figure 2C). Digestion of the PCR product will indicate the presence of the restriction site and stop codon. The genotype was verified by Sanger sequencing.

Results

CRISPR fly generation and screen

2 mutant alleles were previously described to cause shifts to LDCVs and away from SVs, termed *Δ3* and *Y600A*. Both alleles are hypomorphic forms of *DVMAT.* *Δ3* retains some VMAT on SVs whereas *Y600A* has a much more dramatic shift. *Δ3* having an intermediate phenotype was more

reasonable since it may have less severe of a phenotype. It is also possible that *Y600A* phenotype would be as severe as a null mutation and decreased viability.

∆*3* being less dramatic of a change as *Y600A* makes it more likely to have some functions intact [4]. Processes that rely of SV release may have decreased but some function remaining, which can be examined experimentally. The *Y600A* being more dramatic may result in total dysfunction of circuits and functions reliant of SV release. ∆*3* being an intermediate phenotype is advantageous. This also allows for experiments that can tease out subtle differences that cannot be done with *Y600A* if the phenotypes are so dramatic that it is like *DVMAT-null*. There is good chance that this is in the case since the rescue experiments with *Y600A* did not restore fertility in null mutants and overexpression caused dysfunction in wild-types [4]. Work on *Y600A* has since been taken up by others in the laboratory.

The design of the mutagenesis is focused on the last exon of *DVMAT* (Figure 1B).

The intended mutation will accomplish

- Stop codon – truncation of C-terminal trafficking signals
- Only *DVMAT-A* affected, *-B* form is preserved
- Produce BglII restriction digest site – for molecular genotyping
- Mutation of PAM and seed sequence – prevent cleavage of donor or re-cleavage of genome

To follow the mutant locus, I designed a PCR reaction for a ~1040bp region across the mutation site. Cleavage by BglII into two bands (approx. 460 and 580bp) signifies the presence of the mutation on the 2R chromosome *DVMAT* locus (Figure 2C).

The mutation is introduced to the locus by homologous recombination. A single-stranded oligodeoxynucleotide (ssODN) of 90-bp in length was designed to span across the cut site. The ssODN carried a sequence that mutates the locus into a stop codon, a BglII restriction site, and

mutation of the PAM site. The stop codon achieves the intended mutation, the BglII site is used for molecular genotyping by PCR and restriction digest, and the PAM site mutation is to prevent cutting of the ssODN. The ssODN and the gRNA vector were injected into vas-cas9 flies, creating germline mosaics (Best Gene, Chino Hills, CA). The germline mosaics were then used to sample 5 flies to create fly lines.

The process was as follows (Figure 2A):

- About 100 flies injected by Best Gene. With the genotype *CR*/+, where *CR* is the mutation and + is wild-type.
- Sample as many germline mosaics as possible
- Sample 5 progeny from each germline mosaic.
- 450-500fly lines/crosses to create stable lines of candidate mutants
- Phenotypic screen

57 total fly lines from 17 germline mosaics lines showed phenotype and were screened by PCR, digest, sequencing

23 positives from 10 germline mosaics

Germline mosaics gave rise to different genotypes including the full correct mutation, mutation lacking PAM site changes, insertion/deletions/frameshifts, and completely unaltered locus. The difference from full mutation and lacking the PAM site changes is likely due to the design of the repair.

The ultimate reason for creating the *Δ3* mutant is for recombination with transgenes for OA signaling experiments. This requires recombination of the *DVMATΔ3* locus with the transgene insertion, where ever it may be. *DVMAT* is located on the 2R chromosome. Unfortunately, the

TDC2-GAL4 and *TDC2-LEXA* drivers are both on the 2nd chromosome. Any recombination with the *DVMATΔ3* is done with the same fly screen as the original mutagenesis.

TDC2-GAL4 is at an unknown insertion site whereas *TDC2-LEXA* insertion is located on a known landing site of the 2L arm. The success rate of recombination from 2R and 2L across the centromere is 50%.

Recombination rate for *DVMATΔ3* and *TDC2-GAL4* depends on the distance of the loci on the same chromosome and the likelihood of crossover events.

I spent a large effort and a lot of time dedicated to this recombination. *Δ3, TDC2-GAL4* had a 4% recombination rate and *Δ3, TDC2-LEXA* had 50% recombination rates in my screen. These two fly lines are very valuable for experiments involving OA signaling.

Although mutation was easier by ssODN, it does not have the convenience of a visible marker like dsRed insertion from a plasmid donor. For every step, *DVMATΔ3* must be followed by molecular genotyping.

Discussion

Through multiple iterations, I was able to create the *DVMATΔ3* mutation by optimizing the fly-husbandry, molecular genotyping workflow, and thoughtful gene editing design. The initial trial was a failure in that I received very few potential germline mosaic flies from the injection service. With only a few flies, I did not find any mutants of any kind. In the 2nd trial, I was able to generate *DVMAT* mutants that were indel and frameshift mutants. This indicated the 2nd guide RNA target site was successfully cleaved however it did not incorporate the intended mutation. This suggested that the repair ssODN template may be problematic. I used an ssODN of 200 nucleotides in length. While this is the suggestion made by many CRISPR resources at the time, I had no success in homology directed repair. Some studies have shown that HDR efficiency is a function of nucleotide length and symmetry [7]. Maximum efficiency was achieved with 90

nucleotide ssODNs, where symmetry of homology arms was a less important factor. With this in mind, I rationalized that the length probably results in complex secondary structure where the ssODN self-anneals and no longer accesses the genome while folded. A shorter ssODN may alleviate some of these problems where fewer nucleotides are less likely to fold. This resulted in a very productive 3rd trial.

As previously discussed, this round of mutagenesis resulted in 23 positive fly lines from 10 germline mosaics (from ~100 injected larvae, sampled 5 times each). Our success rate was dramatically improved by the shorter ssODN. Our phenotypic screen approach proved feasible with an unmarked CRISPR/Cas9 mutation. This screen was somewhat anticipatory of the phenotype, looking for clones that have altered female fertility and egg-laying. This approach would not have been possible if there was no phenotype from the previous rescue experiments. I have demonstrated that CRISPR/Cas9 mutants of particular design, such as a well-studied allele, can be created with a simple homology directed repair template. This saves a lot of work up front compared to the DNA plasmid that delivers a much larger insertion. The tradeoff is that this screen must be done by phenotype and then genotyped by PCR and restriction digest and Sanger sequencing at the end of the pipeline. In addition, any type of following of the chromosome during recombination must be followed and verified molecularly.

Shortcomings. Recombination by PCR genotyping proved to be a major rate-limiting step for experiments. Mutant experiments could not begin until the allele was recombined with transgenic fly lines used for experiments. I have also forgone outcrossing for my experiments in the interest of time. This emphasizes the importance of thoughtful mutation design and foresight of experiments to test that mutation.

Δ*3 dsRed*: successful mutagenesis, imperfect repair template

I also created an alternative mutant as a back-up strategy [6]; however, the previously mentioned mutant better suited my needs. Potential mutant recombinants include a PxP3-dsRed cassette that causes expression of the fluorophore in the flies' eyes. This marker could then be "hopped out" and leave behind a perfect ∆3 mutant. Ultimately, the previously described strategy yielded me the desired mutation but this alternative strategy did not because of shortcomings of my design.

Eventually I was able to clone a construct by Gibson Assembly that had 1kb homology arms that carried a *DVMAT∆3* stop codon and restriction site for genotyping and the dsRed marker. The creation of the homology arms by PCR and Gibson Assembly cloning proved to be extremely difficult.

I created this donor repair plasmid by cloning homology arms that flank the mutation site by PCR of the vas-cas9 fly. The PCR constructs were then modified by PCR amplification with different primers that would add the mutation to the DNA strand. These 2 homology arms were then ligated by a Gibson reaction to the parent vector (pHD-scarless-dsRed). At the time I considered this mutagenesis a success, however I overlooked the quality of the homology arms I created.

Following cloning of the dsRed repair construct, this DNA was injected into vas-cas9 flies (Best Gene, Chino Hills, CA). Potential recombinants were screened by eye color. These flies were then genotyped by PCR and restriction digest (HindIII). This resulted in 2 germline-mosaic fly lines, each giving rise to 5 founder lines each (founders being progeny who are somatic mutants). All 10 had the dsRed and mutation incorporated into the genome.

The major problem is that when I created the repair construct, I overlooked issues like the 3'UTR disruption and missing segment from the Gibson assembly cloning. When I Sanger sequenced the locus, I realized there are missing 400 bases, disrupting the 3'UTR.

This fly is useless as it does not create ∆*3* mutation, but I kept the fly lines in case of newfound use. It probably has errors for the 3'UTR for both A and B, and thus unstable transcript. That may explain the phenotype of full infertility, no eggs laid at all like the full *DVMAT-null* allele. This in contrast to the ssODN fly successful mutants that have non-zero fertility and egg-laying. The mutagenesis was successful, however the construct I created was incorrect.

I have since designed a new approach to mutate *DVMAT* with updated CRISPR/Cas9 approaches.

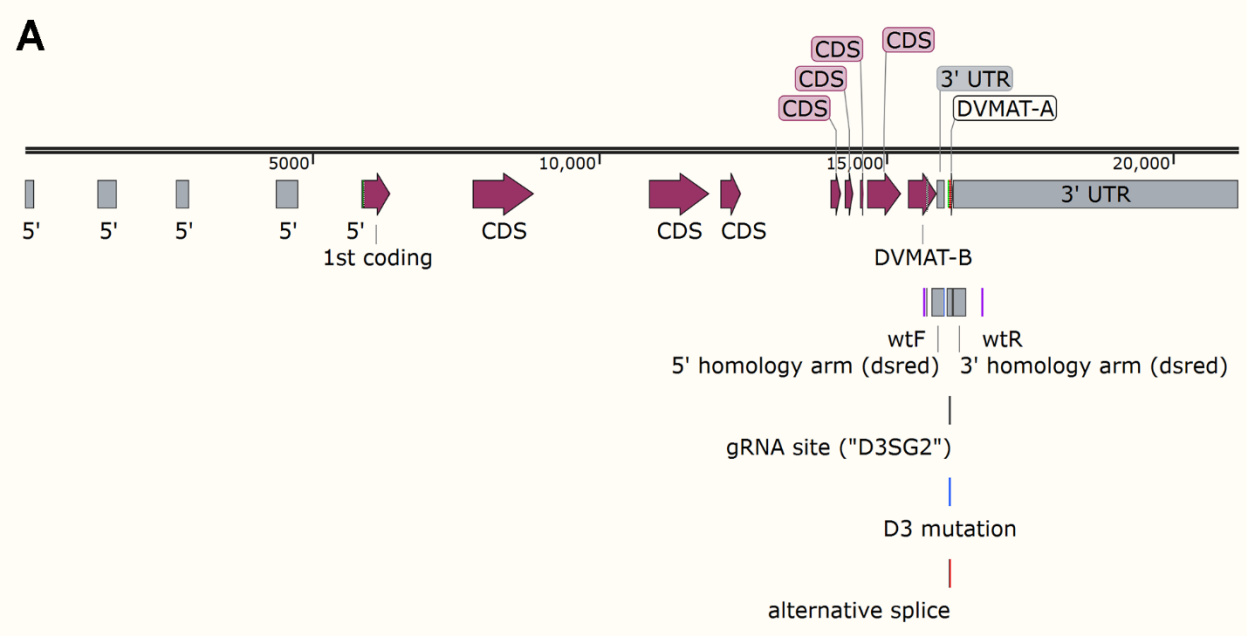

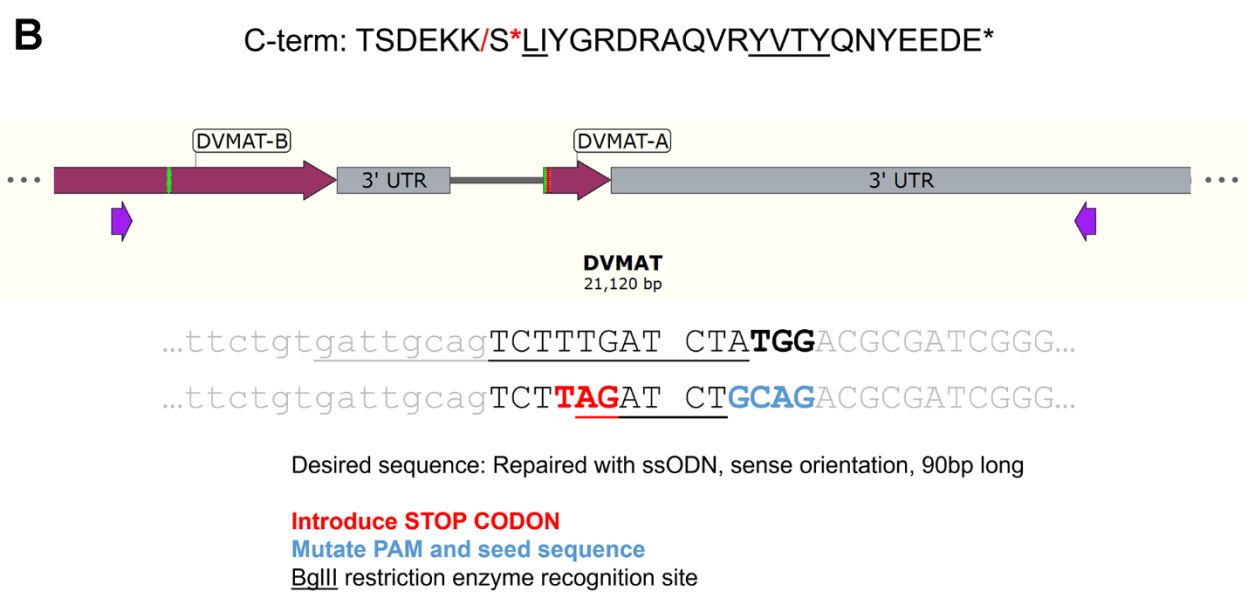

Figure 1. *DVMATΔ3* CRISPR/Cas9 mutagenesis design

A. *DVMAT* gene full length displayed. Each block represents exons and space between represents introns. Grey blocks represent both 5' and 3' untranslated regions. Magenta block arrows represent coding sequence. Regions marked dsRed denote homology arms in Δ3-dsRed construct. At the 3' end of the gene, *DVMAT-A* and *DVMAT-B* exons are

targeted by guide RNA "Δ3SG2". This site is the design of both single-stranded repair and plasmid (dsred) repair designs. wtF and wtR are PCR primers for genotyping. The *Δ3* mutation will be introduced precisely after the alternative splice site for *DVMAT-A* and *DVMAT-B* final exons.

B. C-term representation of DVMAT C-terminal trafficking domain. Amino acids are represented here in single letter code. Underlined symbols are the dileucine motif and the tyrosine-based motif. Red slash represents the original *Δ3* truncation. *Y600A* is a mutation of the tyrosine-based motif. Red asterisk denotes the intended stop codon to be introduced by CRISPR/Cas9 mutagenesis.

Enlarged locus of *DVMAT-A* and *DVMAT-B* exons encoding for their corresponding C-terminal trafficking domains. The final exon can be alternatively spliced at the green marker. The red marker represents the intended mutation site.

DNA sequence. Top line: Wild-type DNA code. Underlined is guide RNA sequence. Bold is the PAM sequence. Space represents the cut site by Cas9. Bottom line: desired sequence for *Δ3* mutagenesis. Red represents intended mutation of TAG stop codon. Space represents cut site. Blue represents Mutate PAM and seed sequence. Underlined is BglII restriction enzyme recognition site.

A

$\frac{CR}{+}$ x $\frac{Tft}{CyO}$ → select CyO flies

? = CR or +

$\frac{?}{CyO}$ x $\frac{Tft}{CyO}$ → select $\frac{?*}{CyO}$
isolated chromosome (clonal)

$\frac{?*}{CyO}$x $\frac{?*}{CyO}$ → stable fly line

Test cross
$\frac{?*}{?*}$ x any fly → Screen for infertility in $\frac{?*}{?*}$ females

~100 flies injected – **germline mosaics**
Sampled 5 flies of each line
Total of ~450-500 fly lines made

RESULT
Selecting for female infertility, low # of eggs
~57 fly lines (potential founders)
From 17 germline mosaics

Positive for Δ3 and BglII sites
10 germline mosaics yielding at least 1 founder
23 founder lines

B

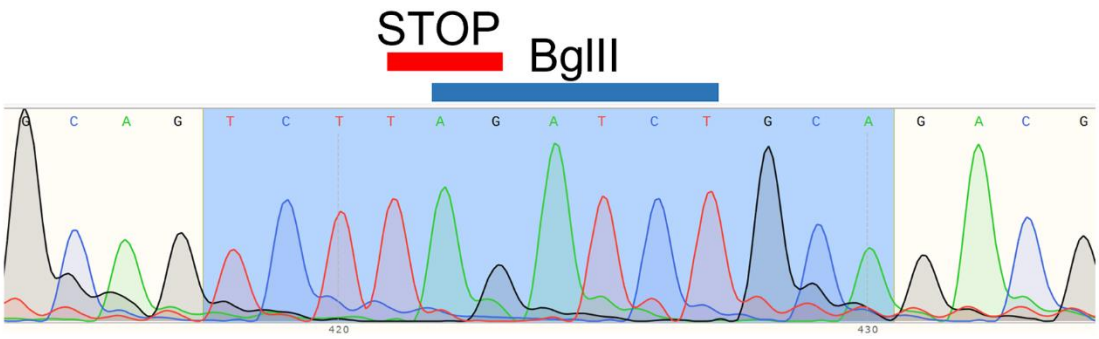

C

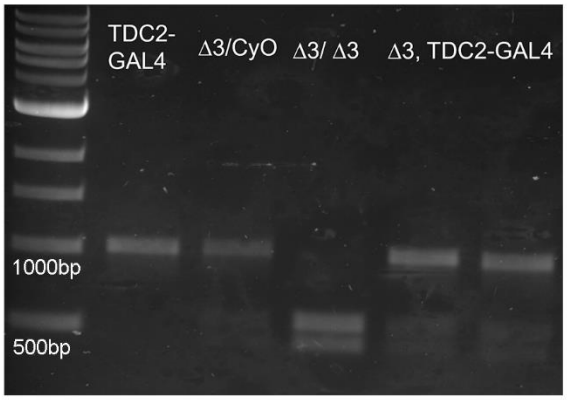

D

F8A – Δ3

cagTCTTTGATCTATGGACGCGATCGGGCTCAGGTACGTTATGTAACCTATCAAAACTACGAGGAAGACGAATAA
cagTCTTAGATCTGCAGACGCGATCGGGCTCAGGTACGTTATGTAACCTATCAAAACTACGAGGAAGACGAATAA
stop BglII

S*

exact match to 90-nt ssODN, positive Δ3 mutant

F7B – WT

cagTCTTTGATCTATGGACGCGATCGGGCTCAGGTACGTTATGTAACCTATCAAAACTACGAGGAAGACGAATAA
cagTCTTTGATCTATGGACGCGATCGGGCTCAGGTACGTTATGTAACCTATCAAAACTACGAGGAAGACGAATAA
SLIYGRDRAQVRYVTYQNYEEDE*

F24D

cagTCTTTGATCTATGGACGCGATCGGGCTCAGGTACGTTATGTAACCTATCAAAACTACGAGGAAGACGAATAA
cagTCTT----CTATGGACGCGATCGGGCTCAGGTACGTTATGTAACCTATCAAAACTACGAGGAAGACGAATAA
SSMDAIGLRYVM*

4-nt deletion, frame shift

Figure 2. *DVMATΔ3* CRISPR/Cas9 results

A. Genetic crosses for generating mutant fly lines via single-stranded repair.

B. Sanger Sequencing chromatogram example demonstrating precise editing that introduced the intended stop codon and restriction digest site.

C. PCR and gel electrophoresis with wtF and wtR primers and restriction digest by BglII. Cleavage of DNA into 2 short products indicates the presence of a *DVMAT*Δ*3* mutant chromosome.

D. Examples from generated fly lines. Sample ID, DNA code compared to wild-type, and translational product

E. F8A is a positive Δ*3* mutant with stop codon, BglII site in place. Translates to serine followed by stop

F. F7B is a wild-type fly that came through the mutagenesis process. DNA code remains unchanged and translates to the DVMAT-A C-terminal trafficking domain.

G. F24D is a deletion and frameshift mutation. DNA code shows missing bases and is translated into a different amino acid sequence.

Chapter 2

Octopaminergic neuronal innervation of female reproductive system

Key Points

Hypothesis: OA neurons in the abdominal ganglion have specific patterns of innervation of the female reproductive system.

Results: 9 OA neurons target specific organs and domains in the reproductive tract. The pattern is segmental and regional, but not tiled. These findings suggest several functions of OA, key roles of each neuron, and coordinated activity to drive ovulation.

Introduction

OA neurons in the abdominal ganglion were previously described to innervate the female reproductive system [8]. Ventral, unpaired, midline neurons are labeled by *TDC2-GAL4* and reside as a column of cell bodies in the abdominal ganglion (Figure 4A, 5A) [8, 9]. Their axons exit the ventral through the abdominal nerve and innervate both sides of the body (Figure 4D).

These neurons are pseudo-unipolar like many fly neurons. The single process from the cell body dives dorsally and bifurcates to form 2 bilaterally symmetric dendritic fields and axons (Figure 4C, 5A). The 2 axons then branch and innervate their respective sides of the female reproductive system. The innervation of the reproductive tract is extensive, with coverage of all of the organs (Figure 4D): ovaries, lateral and common oviducts, uterus, seminal receptacle, spermathecae, and paraovaria.

Although, many functions of OA in the reproductive system have been previously described [8], the detailed neuroanatomy and source of OA are poorly understood. It is important to understand the nuances of anatomy to guide experiments that test the function of OA.

Using stochastic labeling and visualizing both the abdominal ganglion and reproductive tract, I determined the innervation patterns and domains of 9 OA neurons. Multi-Color Flp-Out (MCFO) is labeling technique that stochastically expresses multiple epitopes in a GAL4 pattern [10]. This technique is useful in both isolating a single neuron to trace its innervation and densely labeling multiple neurons to understand their spatial relationships. Combined with a standardized map of *TDC2-GAL4 UAS-mCD8::GFP* (Figure 4A, 4B), I mapped 9 neurons onto their target organs and/or domains.

Each cell exhibits distinct domains of axonal arborization. These cells map onto all of the organs of female reproductive tract. The domains are segmental and organ specific. Most organs have a dedicated neuron. Some organs/domains receive innervation from multiple neurons. Similarly, 1 particular neuron can innervate multiple organs/domains.

These experiments and data demonstrate that OA neurons innervate the female reproductive tract in a segmental and organ/domain-specific fashion.

Methods and Materials

TDC2-GAL4 adult flies were crossed with the MCFO-7 line [10], which has weak Flpase activity, leading to stochastic labeling of neurons in the *TDC2-GAL4* pattern.

The CNS and female reproductive system of adult female flies (5-7 days post-eclosion) were dissected out in phosphate-buffered saline. The tissues were fixed in 4% PFA in PBS for 30min, washed, permeabilized with 0.1-0.3% Triton X-100 in PBS (PBST). Then the tissue was blocked with 5% normal goat serum in PBST for 30min and incubated with the 3 primary antibodies overnight. Primary antibodies probed against the 3 epitope tags HA, V5, and FLAG. The tissue was washed and incubated with secondary antibodies for fluorescent signal amplification. The tissue was cleared using mounting media. The labeled cells were visualized by confocal microscopy.

Ideally, flies were mounted in a position to visualize the ventral surface of the abdominal ganglion and preserve as many connections as possible.

The different target organs and domains were defined in early experiments. Without regard to the neuron cell bodies in the abdominal ganglion, I found the distinct axonal arborizations as they mapped onto the reproductive organs.

The individual neurons and their cell bodies were assigned to their corresponding innervation domains by color matching the axonal arborizations with the cell bodies in the abdominal ganglion.

In single labeled preparations, the assignment is straight forward however it does not demonstrate the spatial arrangement since no other neurons are labeled.

In densely labeled preparations, the spatial arrangement within the ganglion was determined by comparing densely labeled preparations to a standardized map of the abdominal ganglion. Previously mapped neurons were marked as such and the remaining neurons were mapped more easily.

Although there is sometimes variation of the positions of cells across individual animals, it can be primarily attributed to technical performance of dissection and immunofluorescent staining. The nervous tissue is fragile and the cell bodies are on the surface of the ganglion. The arrangement presented here is the best approximation of the position of cells based on this process.

Results

Mapping of 9 cells and determining their axonal arborization domains.

From anterior to posterior

The anterior structures of the female reproductive tract are the ovaries, lateral oviducts, and calyces (the junction between). 3 neurons are responsible for innervation of these 3 structures. Their axons travel together and then branch proximal to the calyces (Figure 6B, B', F, F', F''). The

centered, most anterior neuron innervates the calyces (Cal). 2 neurons lay just posterior to the Cal neuron, the left innervating the ovaries (Ov) and the right innervating the lateral oviducts (LO).

The next structure of the reproductive tract is the common oviduct. A single neuron innervates both the lateral oviduct and the anterior ~2/3 of the common oviduct (LO+COa) (Figure 6A, 6D). Similarly, another single neuron innervates both the posterior ~1/3 of the common oviduct, the anterior uterus, and the seminal receptacle (COp+Uta+SR) (Figure 6A, 6C).

The uterus itself has 2 different neurons responsible for innervation. The 1st neuron is the previously described COp+Uta+SR neuron (Figure 6A, 6C) and the 2nd neuron innervates the posterior Uterus (Utp) (Figure 6C).

The accessory organs are also targeted by the cluster of neurons. The spermathecae receives projections from 2 different neurons (SpA and SpB) (Figure 6E) while the paraovaria glands are innervated by a single neuron (Pa) (Figure 6D).

Ovaries, Lateral Oviducts, Calyces

By: Ov LO Cal neurons

Ovulation from the ovary into the lateral oviducts requires coordination of muscular contractions and relaxation to change conformation and drive egg transit. The ovary, lateral oviduct, and calyx is a site where OA has multiple effects across different cell types. It is unclear how these 3 neurons act to drive expulsion of an egg into the lateral oviduct.

Oviduct

By: LO LO+COa COp+Uta+SR neurons

The oviduct is often treated as a single, uniform organ. The anatomical descriptions usually divide the Y-shaped muscular structure into the lateral oviducts and the common oviduct. The boundaries of the two may be arbitrarily delineated. However, the function and finer anatomy

may not match our predicted boundaries. Here in the oviduct, 3 neurons innervate different domains.

Although the lateral oviducts have been labeled individually, I have never observed the anterior common oviduct to be labeled alone. This suggests that the neuron covering the anterior CO also innervates both lateral oviducts.

Uterus

By: COp+Uta+SR Utp neurons

The uterus is innervated by 2 neurons, presumably dividing the uterus into anterior and posterior. The anterior neuron innervates 3 structures (COp+Uta+SR) and may govern activity for a process requiring all 3 to be co-regulated in time.

The posterior neuron (Utp) innervates the posterior region. However it is unclear how the 2 neurons differ. It possible that 1 neuron (COp+Uta+SR) is involved in control of lumen size and generating force whereas the other (Utp) may be controlling the conformation of the uterus.

Accessory Organs

Seminal Receptacle

By: COp+Uta+SR neuron

The seminal receptacle is innervated by a neuron that covers the 3 structures. This region, although composed of different organs, must be regulated together. This junction of the oviducts, uterus, and accessory organs is the site of many processes.

Spermathecae

By: SpA SpB neurons

The spermathecae receive axon terminals from 2 different neurons. These two neurons are not adjacent in the abdominal ganglion, however their axon terminals on the muscular stalks of the spermathecae are interspersed. It is unclear why two separate neurons would both make synapses adjacent to one another.

Paraovaria

By: Pa neuron

The paraovaria glands have their own independent innervation.

Tiling, Segmental, Organ/Domain specific

The data shown here demonstrate that the neuronal innervation of the female reproductive tract is segmental and organ specific. The innervation is not tiled. The domains do not have a regular shape, do not meet edge-to-edge, and sometimes overlaps. Regardless, this level of specificity is achieved by dedicated neurons to different portions of the reproductive tract. Here, I present a model of OA innervation of the female reproductive tract (Figure 7). This cluster of OA neurons in the abdominal ganglion have diverse and distinct targets of innervation. These particular innervation patterns are suggestive of different functions at each site. Previously, this group of neurons was described to innervate every part of the reproductive system. However, the detailed neuroanatomy reveal that the action of OA is far more complex than previously thought.

Discussion

These distinct innervation domains are suggestive that each neuron bears heavy influence on its corresponding target organ. In addition, these neurons may be responsible for individualized regulation or modulation of target organ activity. This implies that the various functions of OA are in part controlled by anatomically distinct neurons.

Moreover, this complex of neurons of a single type interfacing with a diverse set of targets represents a model of parallel OA signaling streams. I hesitate to use the term “synapse” as it is unclear whether release of OA is done from synaptic vesicles at an axon terminal to a specific post-synaptic site or structure. These parallel signaling streams may be part of a larger coordinated activity to orchestrate organ function.

Given that ovulation is a sequential process down the reproductive tract, it is reasonable that activity of OA neurons is coordinated with some sort of sequential pattern. In addition, the activity of accessory organs may be synchronized to a certain point of ovulation. These issues of activity patterns can be investigated by optogenetic experiments.

Egg transit – gating, egg movement, conformational changes

The muscular structures of the tract are responsible for transition of the egg. Their functions may include contraction and relaxation for squeezing, positioning, and forcing an egg through the tract. It is unclear what each neuron does to the conformation of the organs. The specific innervation suggests that each segment may serve a particular function. For example, at the calyx an egg must be squeezed out of the ovary and expelled into the lateral oviduct. The activity at the calyx required for transit could be relaxation to accommodate the egg while the ovary contracts.

Differential receptor expression – further complicating signaling streams

There are 6 OA receptors that have been described in the literature. I have done preliminary mapping of 5 receptors described here (Appendix A2). Their distribution across cell types and regions further complicates OA signaling streams.

This work has since been picked up and expanded upon by others in the lab.

OAMB receptor is expressed in epithelia throughout the common and lateral oviducts.

OctB2 receptor has a different pattern of expression. Instead, the receptor is expressed in only the lateral oviduct epithelia and fine neuronal-like processes in the distal common oviduct.

OctB1 and OctB3 receptors are expressed in small local cells that have processes throughout the reproductive tract. Their identity and function are yet to be determined.

Oct/Tyr receptor is also shown to be expressed in neurons in the abdominal ganglion (not shown here).

It is important to note that the receptors are not located on the muscle cells themselves. These and other experiments in the lab demonstrated expression in non-muscle cells like the epithelia and local small neurons. Which cells receive OA input, mode of neurotransmitter release, and the specific role at a given site is a major avenue for future studies.

At first, I had an NMJ-like model of synapse for OA neurons onto the muscle of the oviduct. The data obvious shows otherwise. However it suggests that there is some intermediate steps of signaling between the neuron, receptor-expressing cells, and ultimately the oviduct muscle. For monoamines that signal onto GPCRs, any number and type of metabolic processes that can mediate the OA and eventual muscle reactions.

Signaling motifs – from neurons, to organ, to cell, to receptor

At a given site in the reproductive tract, there exists axonal terminals by a particular neuron, and certain receptors expressed in specific cell types. This can be thought of as a signaling motif. Each region may have a particular motif and in turn each motif may have a particular function. Sites where the motif may change from the adjacent site may represent a functional boundary where regulation and effects of OA processes may differ. For example, in the lateral oviducts both OAMB and OctB2 receptors are expressed in epithelia. However, in the common oviduct only OAMB is still expressed in epithelia. It is possible that the difference between the two regions signifies a change in function of and response to OA.

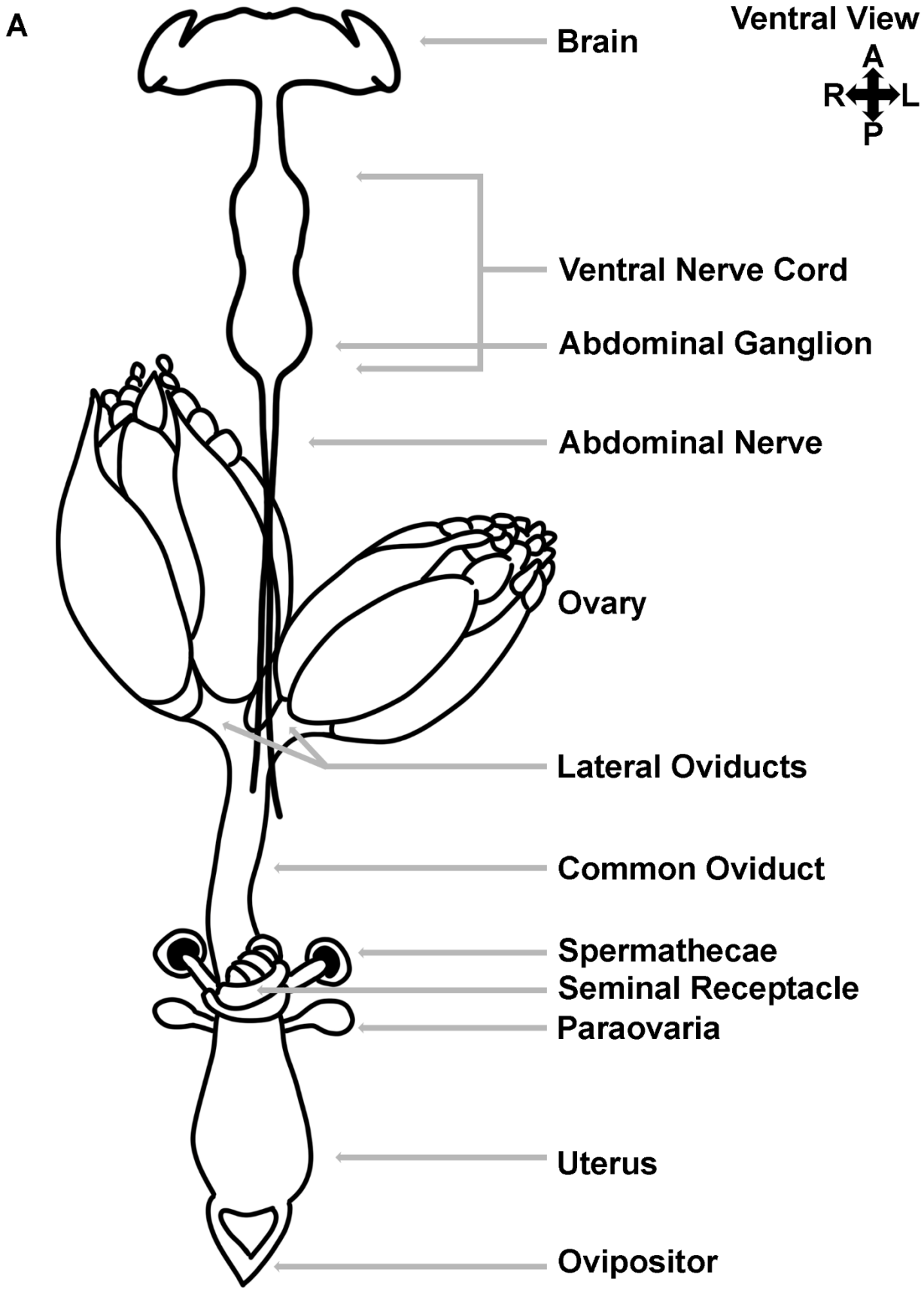
A
Brain
Ventral View
A
R
L
P
Ventral Nerve Cord
Abdominal Ganglion
Abdominal Nerve
Ovary
Lateral Oviducts
Common Oviduct
Spermathecae
Seminal Receptacle
Paraovaria
Uterus
Ovipositor

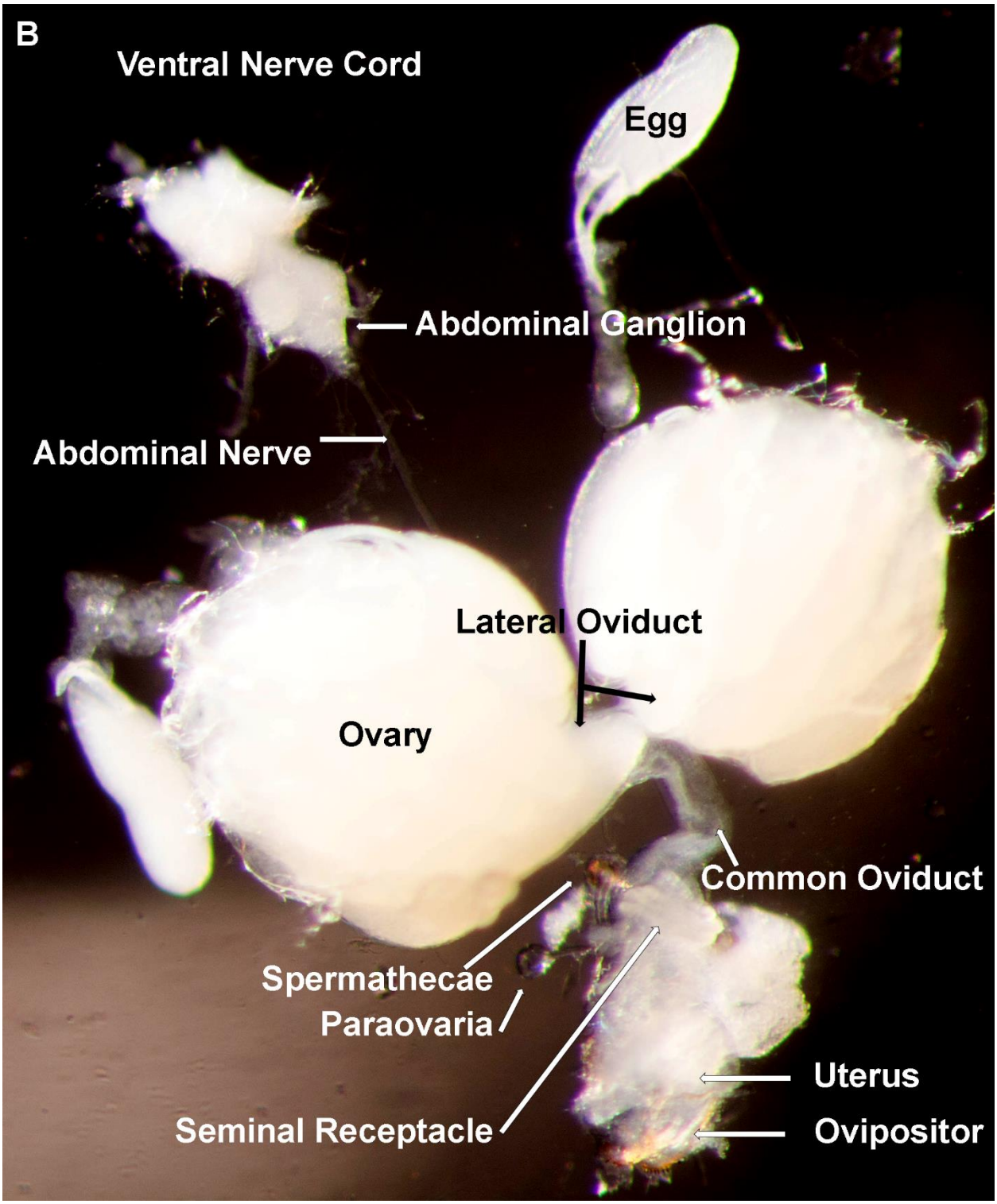

Figure 3. The anatomy of the *Drosophila* central nervous system and the female reproductive tract.

Cartoon (A) and actual specimen (B)

The central nervous system consists of the **brain** and **ventral nerve cord**. The **abdominal ganglion** resides at the posterior end and innervates the contents of the abdomen, including the gastrointestinal and reproductive tracts. Axons coalesce to form the **abdominal nerve** and exit out the posterior pole of the ganglion. The abdominal nerve carries axons (loose ends depicted here) that cover the female reproductive organs.

The female reproductive tract consists of muscular structures and accessory organs. The muscular structures are involved in egg transit. The **ovaries** produce follicles that are positioned and expelled into the **lateral oviducts**. The two lateral oviducts meet and continue as the **common oviduct** and connect to the **uterus**. Several **accessory organs** are located at this junction. The **spermathecae** and **seminal receptacle** are sperm storage organs. The **paraovaria** are female glands. The uterus then connects to the **ovispositor**, which extrudes the egg onto the fly's chosen substrate.

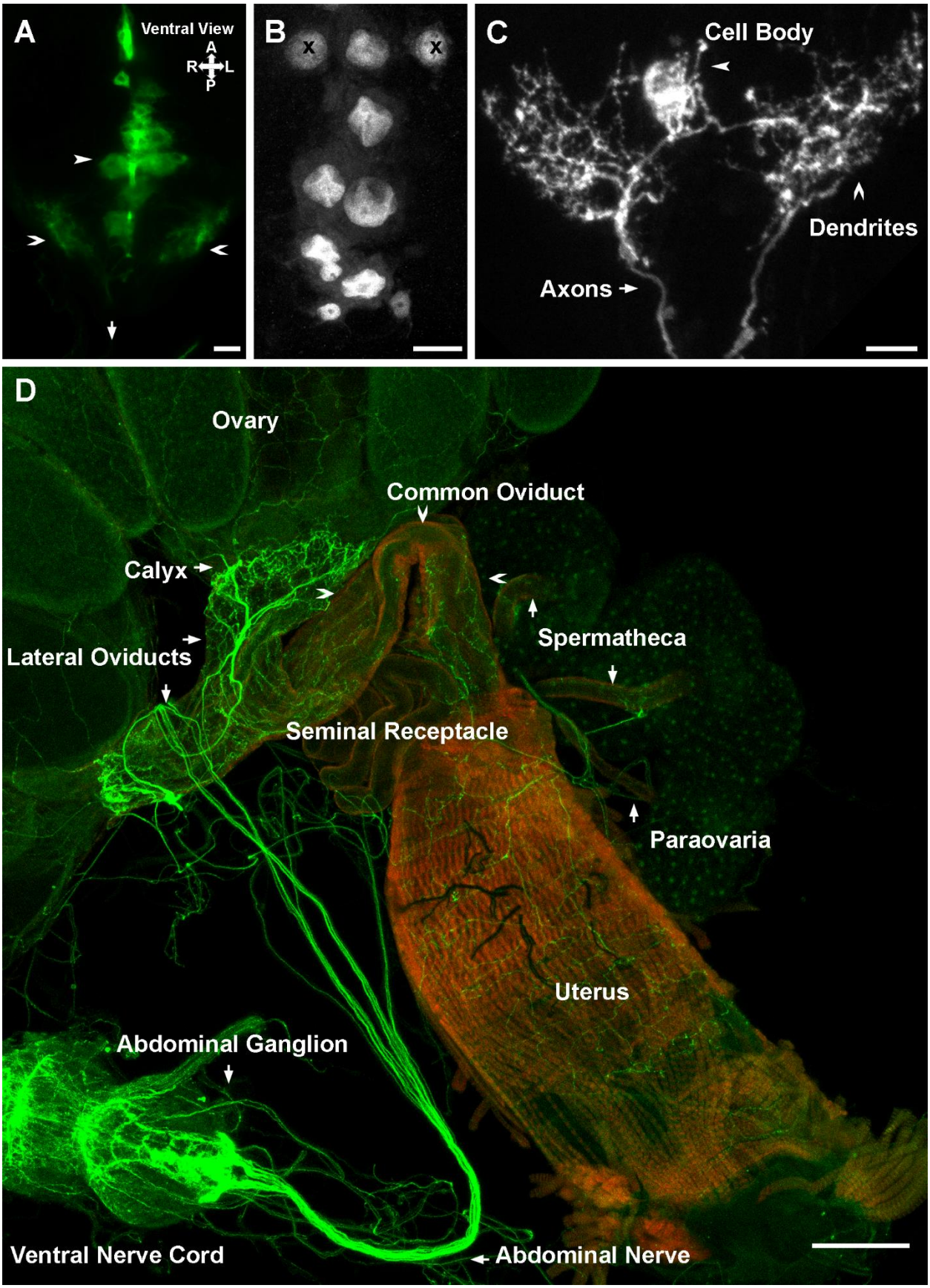
A
Ventral View
A
R
L
P
B
x
x
C
Cell Body
Dendrites
Axons
D
Ovary
Common Oviduct
Calyx
Lateral Oviducts
Spermatheca
Seminal Receptacle
Paraovaria
Uterus
Abdominal Ganglion
Ventral Nerve Cord
Abdominal Nerve

Figure 4. Octopaminergic neurons innervate the female reproductive tract.

OA neurons in the abdominal ganglion send projections that cover all organs and regions of the female reproductive tract.

A. **The cell bodies (arrowhead) are located on the ventral surface, midline of the ganglion**. Each neuron gives rise to 2 dendritic fields (chevron) on both left and right sides and two axons that exit through the abdominal nerve towards the reproductive tract (arrow). (Green = *TDC2-GAL4*; *UAS-mCD8::GFP*) (scale bar 10 microns) (A – anterior, P – posterior, R – right, L – left)

B. **Nuclei of OA neurons.** Their approximate arrangement and spatial relationships are demonstrated by labeling the nuclei. Of 11 neurons shown here, 9 were mapped to the female reproductive tract. (2 neurons shown here have not been mapped (x)). (*TDC2-LEXA*; *LEXAOP-GFP.NLS*)

C. **Morphology of a single OA neuron.** Each neuron is composed a cell body that gives off a single process that then bifurcates into 2 dendritic fields and 2 axons.

D. **The female reproductive tract is heavily innervated by OA neurons and their axonal projections.** The abdominal ganglion is located at the distal pole of the ventral nerve cord. Axons coalesce and form the abdominal nerve exiting the ganglion. The ovaries, lateral oviducts, common oviduct, and uterus are muscular structures that have highly branching and dense OA axons. Accessory organs also receive OA input. These include the sperm storage organs: spermathecae and seminal receptacle, and the paraovaria glands. (Red = phalloidin, Green = *TDC2-GAL4*; *UAS-mCD8::GFP*) (scale bar 100 microns)

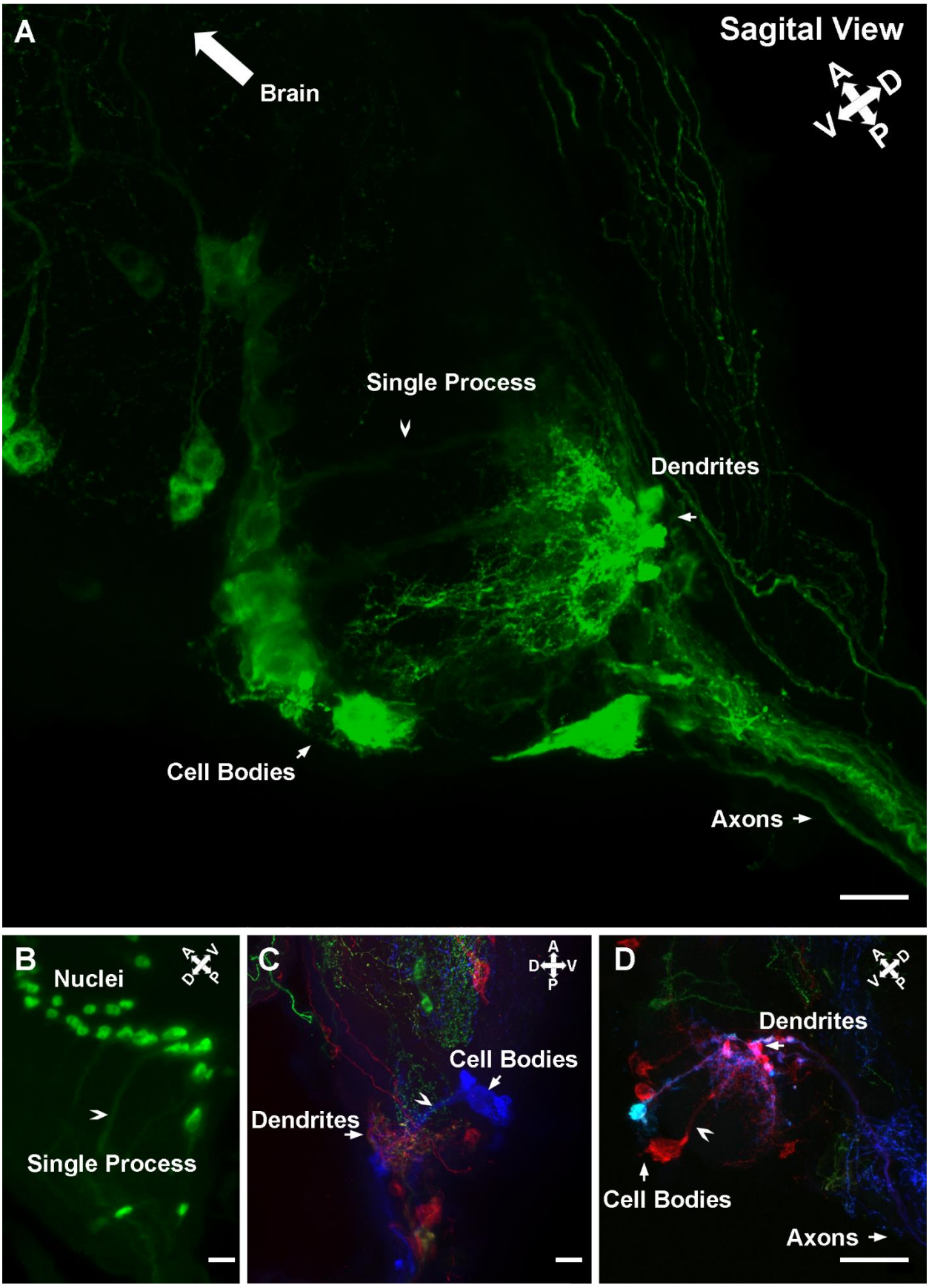
A
Sagital View
Brain
A
D
V
P
Single Process
Dendrites
Cell Bodies
Axons
B
Nuclei
Single Process
C
Cell Bodies
Dendrites
D
Dendrites
Cell Bodies
Axons

Figure 5. Sagittal view of the abdominal ganglion.

A. **OA neuron cell bodies are located on the ventral surface of the abdominal ganglion.** Each cell body projects a single process (chevron) dorsally that then gives rise to two dendritic fields and two axons on either side of the body. (Green = *TDC2-GAL4*; UAS-mCD8::GFP) (A – anterior, P – posterior, D – dorsal, V – ventral)

B. **OA neuron nuclei** demonstrate the individual cells and their corresponding single process (chevron). (*TDC2-LEXA*; LEXAOP-GFP.NLS)

C. And D. OA neurons are situated adjacent to one another on the ventral surface. Their dendrites share the same spatial location and are deeply nested and intertwined. (*TDC2-GAL4*; MCFO)

Figure 6. Multi-color Flp Out (MCFO) labeling and mapping of OA neurons.

OA neurons innervate in a domain and/or organ-specific fashion.

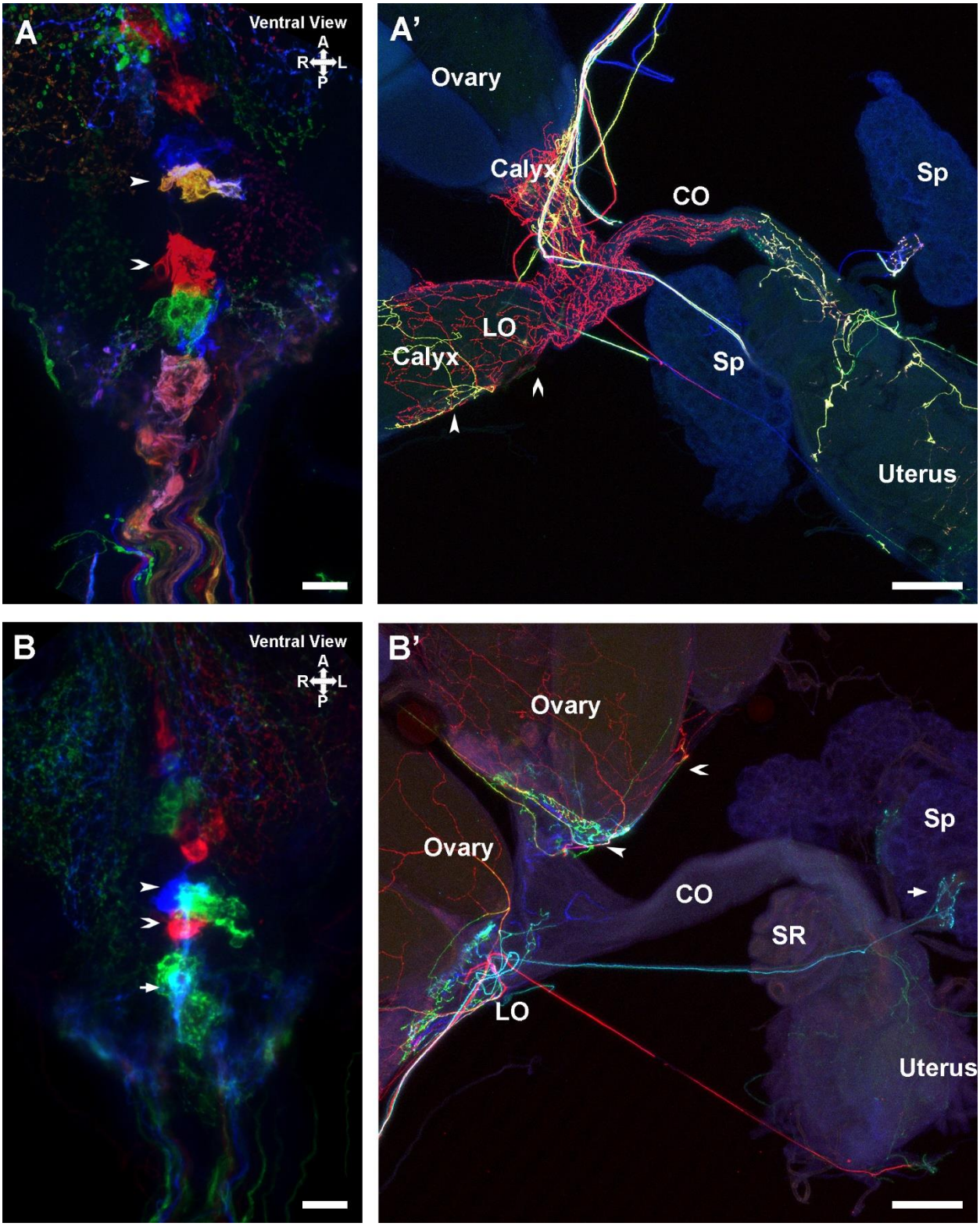
A
Ventral View
A
R
L
P
A'
Ovary
Calyx
CO
Sp
LO
Calyx
Sp
Uterus
B
Ventral View
A
R
L
P
B'
Ovary
Ovary
Sp
CO
SR
LO
Uterus

A and A'. Several neurons are labeled with varying combinations of epitope tags. The anterior, yellow neuron (arrowhead) innervates the calyx (arrowhead) of the lateral oviduct. The lateral oviducts and anterior ~2/3 of the common oviduct are innervated by a single OA neuron (red, chevron). Labeling of the reproductive system demonstrates segmental domains of innervation. The posterior ~1/3 of the common oviduct shares innervation with the anterior uterus.

B and B'. An anterior neuron (red, chevron) innervates both ovaries. (red, chevron). Adjacent are 2 neurons (blue and green) that also innervate the dense region of the calyx. The blue neuron (arrowhead) innervates the lateral oviducts whereas the green neuron is specific to the calyx (arrowhead). More posterior neurons include 2 green neurons that innervate posterior structures. There also lies a light blue neuron (arrow) that innervates the muscular tube of the spermathecae.

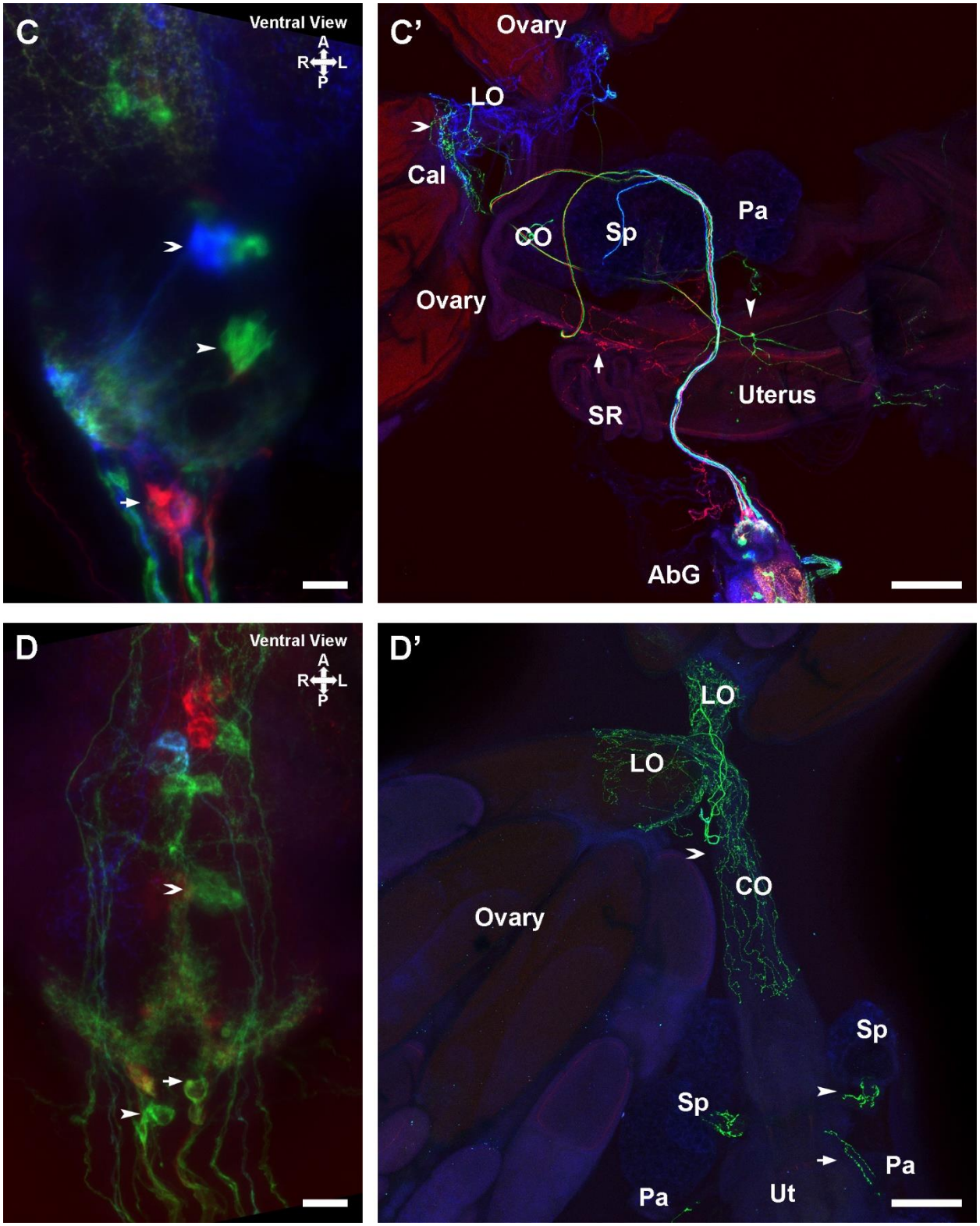

C and C'. An oblique view of the abdominal ganglion. The anterior neurons innervate the lateral oviducts and calyces. The blue neuron (chevron) corresponds to the dense innervation

of the lateral oviducts. The adjacent green neuron corresponds to the thin line of innervation at the calyces. The larger green neuron (arrowhead) innervates the posterior and external portions of the uterus. The red neuron (arrow) is located more posteriorly and innervates the posterior ~1/3 of the common oviduct, the anterior uterus, and seminal receptacle.

D and D'. Three green neurons are visualized here. The large anterior neuron (chevron) innervates the lateral oviducts and the anterior ~2/3 of the common oviduct. A small posterior neuron (arrowhead) on the right side of the body innervates the spermathecae. A second small neuron (arrow) located on the left side of the body and situated dorsally innervates the paraovaria.

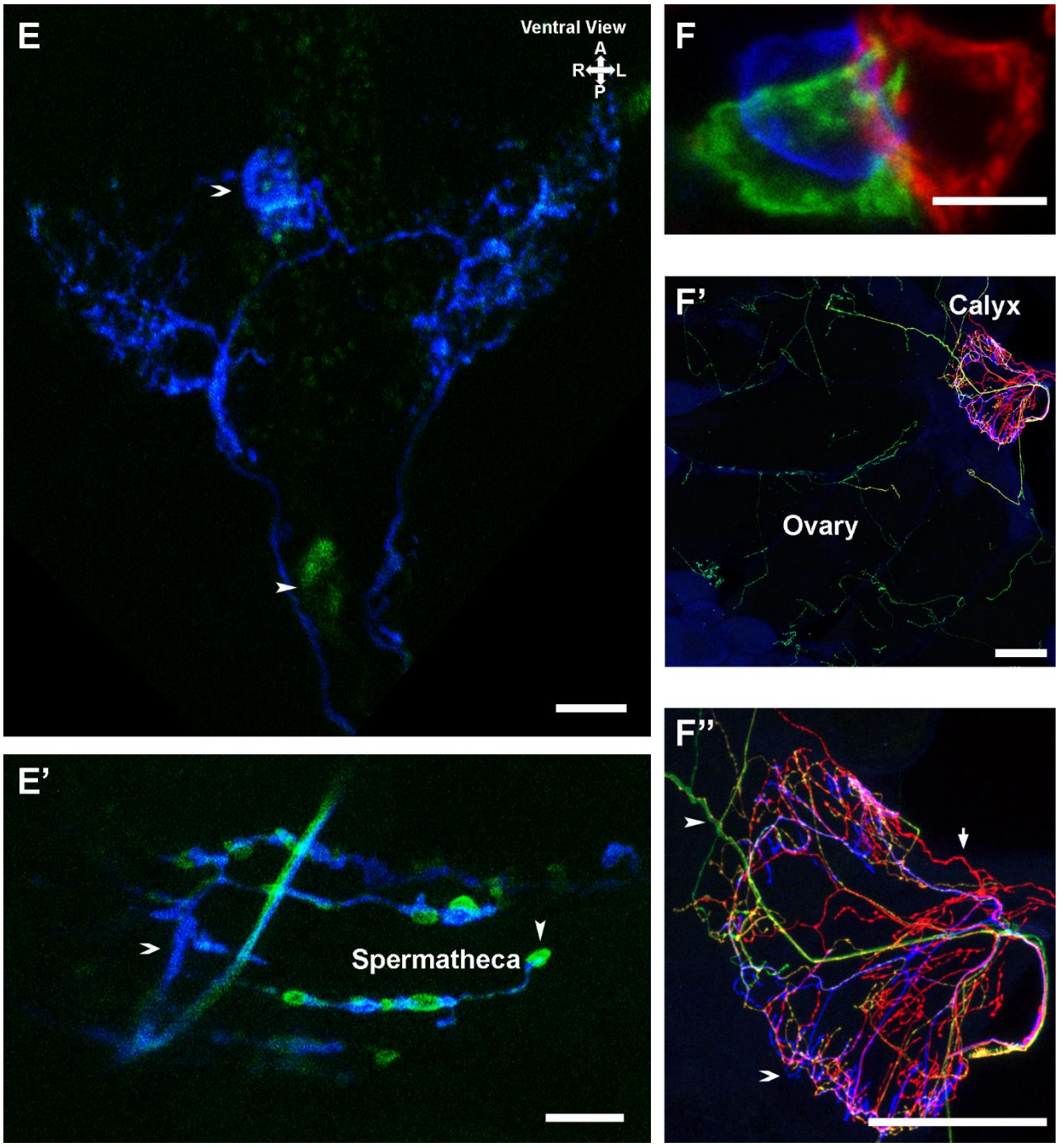

E and E'. Two neurons innervate the spermathecae.

A blue neuron (chevron) innervates both spermathecae. Simultaneously, a small green neuron (arrowhead) also innervates the muscular stalk of the spermathecae. The two neurons have axon terminals that are interspersed with one another.

F, F’, and F’’. Three neurons that are closely situated together at the anterior end of the abdominal ganglion innervate the ovaries (green), calyces (blue), and lateral oviducts (red). These three neurons have axonal projections that overlap however still innervate specific regions. The neurons have axons that travel together that then innervate the ovary (green, arrowhead), the calyx (blue, chevron), and the lateral oviduct (red, arrow).

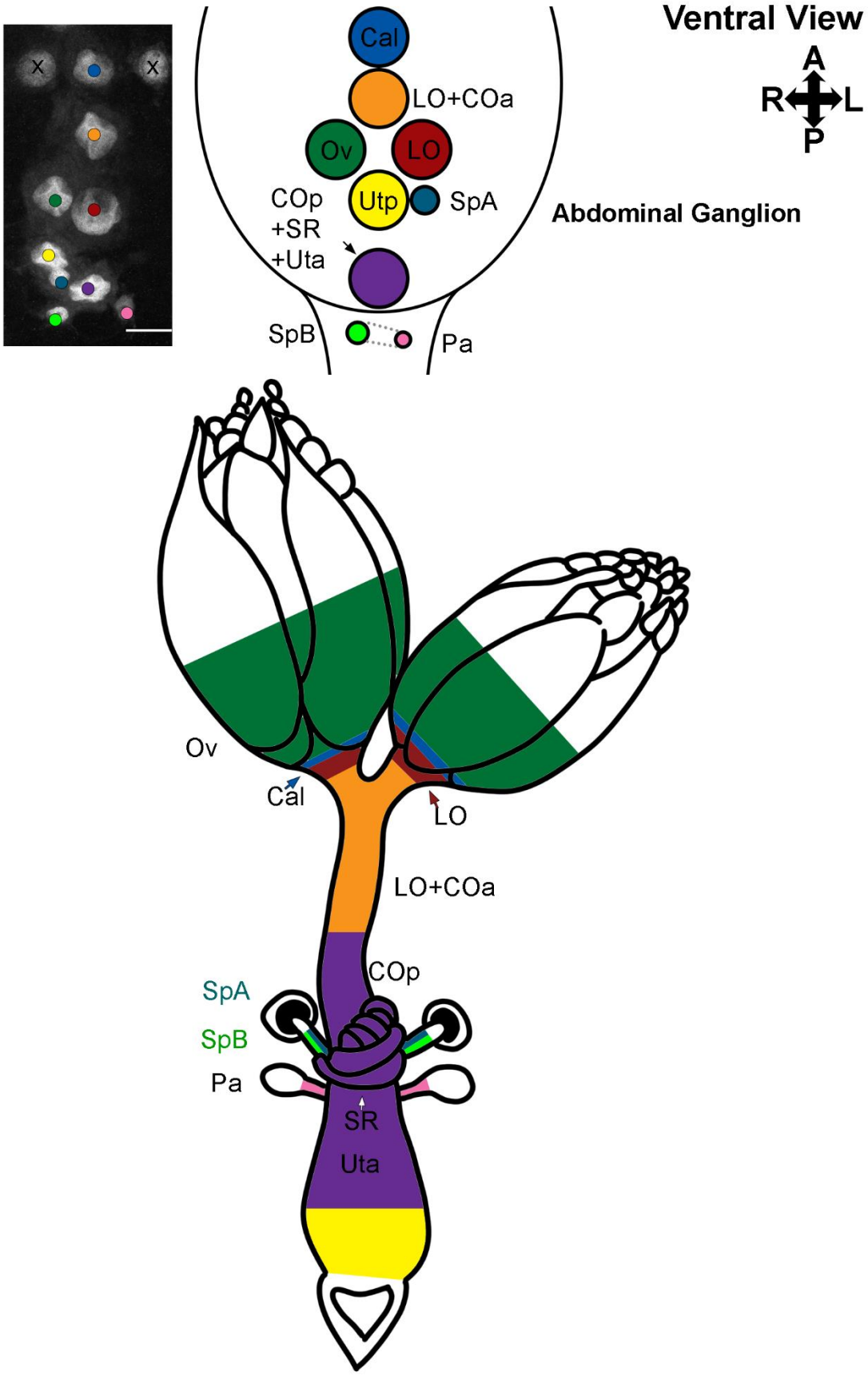
X
X
Cal
LO+COa
Ov
LO
COp
+SR
+Uta
Utp
SpA
SpB
Pa
Ventral View
A
R
L
P
Abdominal Ganglion
Ov
Cal
LO
LO+COa
COp
SpA
SpB
Pa
SR
Uta

Figure 7. Model schematic of the TDC2 innervation of the female reproductive system.

Top: Arrangement of each TDC2 neuron in the abdominal ganglion.

Top left: Nuclei of OA neurons, color-coded to the model abdominal ganglion.

Bottom: Cartoon representation of the female reproductive system.

The colors of each panel demonstrates each neuron and its corresponding organ and/or domain of innervation. Each single neuron bilaterally innervates its domain and/or structures.

Blue: The most superior neuron innervates the calyx (Cal) of the lateral oviducts.

Orange: This midline neuron covers both the lateral oviducts and the anterior ~2/3 of the common oviduct (LO+COa).

Green: This neuron is located on the right side of the body and innervates both ovaries (Ov).

Red: This neuron is located on the left side of the body and innervates both lateral oviducts (LO).

Yellow: A single midline neuron innervates both sides of the posterior uterus (Utp).

Purple: A single large midline neuron innervates several domains including the posterior ~1/3 of the common oviduct (COp), the seminal receptacle (SR), and anterior uterus (Uta).

Navy Blue: This smaller neuron is situation next to the yellow neuron. This is one of two neurons that innervate both left and right spermathecae (SpA).

Bright green: This neuron is located at the posterior end of the abdominal ganglion where the nerve begins. This is one of two neuron that innervate both left and right spermathecae (SpB).

Pink: This small neuron is on the posterior, left, dorsal end of the abdominal ganglion. This neuron innervates both paraovaria glands (Pa).

See appended media for a large poster with further examples of TDC2 MCFO preparations.

Chapter 3

Oviduct Dilation

Key points

Hypothesis. OA causes relaxation of the oviduct.

Results. OA causes multiple actions on the oviduct, including both lateral oviduct contractions and a slow, gradual luminal expansion in the calyces of the lateral oviducts and the anterior common oviduct. Relaxation depends on the OAMB receptor.

Introduction

Control of the female reproductive system involves many neurons and multiple neurotransmitter systems [8, 11-14]. The current model includes a straightforward view: in the oviduct, glutamate causes contraction and OA causes relaxation [12, 15]. However, the early experiments are limited in that they do not examine the oviduct as a more complex organ with distinct regions.

Moreover, the findings are difficult to interpret what is the primary function of OA. Initial studies demonstrating oviduct relaxation were in the context of stimulation of the abdominal nerve with subsequent bath application of OA [12]. These results indicated that OA drives relaxation of the oviduct. However, these experiments do not directly elicit OA functions alone. The abdominal nerve stimulation confounds the action of OA with an unknown number of neurons all active at once. Elucidating the function of a single neurotransmitter cannot be determined in these conditions.

Several experiments in the Krantz Lab have proven that OA causes several effects on the female reproductive system. Sonali Deshpande's work demonstrated that activity of the oviduct driven by OA is far more nuanced and complex. She used the genetically-encoded calcium indicator GCaMP6m expressed in muscle of the female reproductive system (*UAS-GCaMP6m; 24B-GAL4*)

to record contractile activity (Appendix A1). The calcium signal serves as a proxy for contractions based on the muscle physiology of calcium conductance and calcium-induced calcium release from the sarcoplasmic reticulum to drive the actin-myosin contractions.

Whole female reproductive systems were removed from the body and grossly de-innervated by dissection. The tissue was then incubated in HL3.1 standard *Drosophila* media and then OA is applied for a final concentration of 1mM OA in the bath. Activity was recorded by a high-speed fluorescence camera to measure GCaMP signal in the oviduct muscle.

The results are surprising and somewhat contradictory to the published model. OA elicits contractions of the lateral oviducts. This is seen in a burst of large, repetitive, regular contractions. These contractions however are localized to the lateral oviducts.

Further experiments demonstrate that the number of contractions made by the lateral oviduct depends on the function of 2 OA receptors: OAMB receptor and OctB2 receptor. When the number of contractions is compared to their genetic background controls, there is a dramatic decrease in the number of contractions in OctB2 receptor mutants. Similarly, the OAMB receptor mutants decrease in the number of contractions, however with much greater variance (not shown here).

These experiments question the function of a particular neurotransmitter on the female reproductive system as a whole. They are brute-force stimulating the tissue, very far from physiological conditions and activity.

The reproductive system is examined *ex vivo*, the tissue is de-innervated and no neuronal processes are left upon gross dissection. The bath application itself is the extreme stimulation of the oviduct, with issues such as extremely high and constant neurotransmitter presence in the bath. Nonetheless, those experiments assess the maximum response the tissue can surmount

in response to a flood of OA. Although the system is isolated and de-innervated, the tissue likely still has neuron terminals embedded in the muscle.

Neurotransmitter receptors are still functional in their respective cells. From those experiments, we can definitively state that a given neurotransmitter can elicit activity in specific regions of the oviduct. Their action at a given region of the oviduct likely depends on the receptor expression in that organ.

From those experiments, we can conclude that OA is capable of directly stimulating contractions of the lateral oviduct, but not the common oviduct. Furthermore, they demonstrate that the oviduct is not a uniform piece of muscle, congruent with the complex conformational changes the organs of the reproductive system undergo during ovulation.

The reports of OA causing relaxation give us an incomplete model of the primary function of OA [12, 15]. With skepticism of previously assigned function, I investigated whether OA really did cause oviduct relaxation. I conducted the same OA bath-application experiments. On a longer time-scale, OA causes relaxation of the oviduct. Global relaxation occurs over the course of 10min, with a gradual lengthening and widening of the lumen. This dilation of the oviduct demonstrates the validity and incompleteness of the currently-published model.

Here I demonstrate that the female reproductive system responds to OA in multiple ways, including both contraction and relaxation of the oviduct. Using simple visualization by photography, I am able to assess the long-term, global dilation of the oviduct lumen by relaxation. These experiments validate a long-cited notion of OA-driven relaxation [12]. Furthermore, they also prove the multi-faceted action of OA. OA alone can cause two different responses in the oviduct muscle: contractions that shorten the oviducts, and relaxation that dilates the lumen. These two different functions each have a corresponding receptor associated. Contractions

experiments proved that OctB2 receptor is necessary for repeated contractions whereas here I prove the OAMB receptor is necessary or long-term global relaxation of the oviduct.

Methods/Materials

Female reproductive systems were dissected out and isolated from adult female flies (5-7 days post-eclosion). The preparation was dissected and incubated in ice cold HL3.1 standard fly media. The media was refreshed and the preparations were visualized on a Zeiss STEMI SV11 trinocular stereo microscope and photographed with either a Dino Lite eyepiece camera or a Canon EOS DSLR camera. Photographs were taken at 1 frame per second (Dino Lite) or at 1 frame per 5 seconds (Canon).

The entire experiment lasts for 10 minutes. Images were taken to record baseline activity for 1 minute. OA or vehicle control was added to the bath and images were recorded for the remaining 9 minutes.

The tissue was then incubated in HL3.1 standard *Drosophila* media and then OA is applied for a final concentration of 1mM OA in the bath.

Photographic series were imported into imageJ to create a time-series stack image. These photographs were cropped to focus on the oviduct to remove excess image data.

The length across the oviduct is measured before and after OA addition. Measurements are taken across the calyx of the lateral oviducts, the anterior, mid-, and posterior common oviduct. Measurements of the calyx are averages of both sides.

The change in length is represented as $\frac{\Delta L}{L0}$, the relative change in length across a region of the oviduct. It is calculated as $\frac{\Delta L}{L0} = \frac{Lfinal - Linitial}{Linitial}$

In imageJ, the number of pixels is measured across a given anatomical region from edge to edge of the oviduct. Initial and final measurements are taken by averaging 3 replicant measurements.

Genotypes to compare are wild-type flies w1118 and 225 rosey (genetic background controlled) vs OAMB receptor mutant and OctB2 receptor mutant [16-18].

The change in width when imaged from above is an approximation in the dilation and expansion of the volume of the tube-shaped oviduct. A cross section of the oviduct can be roughly estimated to be an ellipse. An increase in length (1 dimension in 2D image) is a proxy for change in major axis length of the ellipse. With the increase in length implies an increase in cross-sectional surface area, and thus an increase in volume that is easily appreciable by eye.

Also, important to note that although some measurements are very small (especially in the mid and posterior CO), they may not obviously reflect dilation in those regions.

However, relaxation may be much more obvious by eye under stereomicroscopy during dissection and clear photography with lighting that exhibits depth and volume. Oviduct width is measured in experiments with clear view of the calyx and entire common oviduct. In the event an egg passes into a space, it is noted and the change in width of the oviduct is taken at a time point before occlusion by the egg.

Results

OA causes luminal expansion in the calyx of the LO and anterior CO

The physical demands of the anterior end (Ovaries, LOs, anterior COs) to passage very large eggs necessitate a much larger volume and relative expansion to accommodate [19]. To investigate this, I isolated female reproductive systems from the body, removing the abdominal nerve and all peripheral nerves attached to the organs (Figure 1A). After dissection, the preparation was transferred to fresh HL3.1. Series of photographs were taken at either 1 frame

per second or 1 frame per 5 seconds. After 1min of recorded baseline activity, OA is added to the preparation for 9minutes at a final concentration of 1mM (Figure 1B). Images are then analyzed by measuring the width across the long axis of the oviduct as it changes before and after OA application. Measurements were taken across the calyx of the LO, anterior CO, mid CO, and posterior CO. The data is expressed as $\frac{\Delta L}{L0} = \frac{Lfinal - Linitial}{Linitial}$, the relative change in width from before and after OA application. This change in width serves as a proxy for an expansion of the lumen of the oviduct. This unidimensional measurement measures the long axis across the ellipsoid tube and serves a proxy of the lumen widening and increasing in volume.

The calyx of the lateral oviduct and the anterior CO exhibit the most dramatic of volume changes following OA addition. At the level of the mid CO, there is some relaxation however it is not captured by the linear measurement. Relaxation of the mid and posterior CO is an opening of the lumen, but not necessarily a widening of across the long axis of the oviduct. The $\frac{\Delta L}{L0}$ measured across the oviduct has the ability to capture large changes (as in calyx and anterior CO).

The anterior common oviduct dilation depends on OAMB receptor

OAMB mutant flies respond to OA with LO contractions, but not the global relaxation. This is most obvious at the anterior CO. WT flies respond to OA with relaxation in the calyx and anterior CO. By contrast in OAMB mutant flies, the anterior CO actually decreases in length, ending in a more contracted state (Figure 2B, 4A). This is probably related to LO contractions that bring it a contracted state, but do not relax over time. This results in an even more contracted state than before OA application.

In OctB2 mutants, there is no appreciable loss of relaxation (Figure 2D, 4B). OctB2 receptor mutants relax to the same degree as their wild-type controls of the same genetic background.

Discussion

These bath application experiments are brute force and far from physiological activity. However, this preparation pushes the effect of OA well to its extreme, allowing us elucidate different effects with clear differences across OA receptor mutant genotypes.

Relaxation may occur at all parts of the oviduct, however not uniformly. The lateral oviducts and calyces and the anterior CO dilate profoundly that it can easily be visualized. The linear measurement may not reflect relaxation in the mid and posterior oviducts.

When considering the complex organ structure and muscle arrangements, it makes sense that there are different forms of contraction and relaxation, depending on the conformations needed during ovulation. Dilation in the calyx may facilitate reception of many prime-positioned follicles from the ovaries. The anterior CO also dilates to large degree and is perhaps related to the same need as the calyx for reception space.

OAMB is needed for relaxation of anterior CO. OAMB flies end up with narrowing of the anterior CO (following episodes of contraction, no global relaxation).

In contrast, flies that are OctB2 mutant do relax. Since OAMB is still expressed in OctB2 mutants, relaxation remains intact. It is unclear if the two receptors conduct 2 different functions or both participate in a single function. This suggests that there is some coordinated activity that is much more dynamic than previously thought.

The receptor mutants have both been described to have decreased egg-laying [16-18, 20], which is a large and complex behavior. In experiments examining oviduct contraction and relaxation, we are able to show that measured infertility and low fecundity reported result from different deficits at oviduct. There may be a variety of reasons why ovulation and egg-laying does not work in these mutants, but we can at least assign relaxation and contraction to two different receptors.

Defects in ovulation can be due to loss of contraction or relaxation, with the net gross behavior of decreased egg-laying.

OA-driven, pulsatile, linear contractions of the lateral oviduct and global, longitudinal dilation of the oviduct lumen are the extreme case of constant OA stimulation over 10 minutes. In these conditions, dynamic signaling is not possible and stimulation of different effects will reflect intrinsic properties of the tissues that express OA receptors. In this case we see that an oviduct will contract in bursts repetitively and cause a observe global relaxation occurs over time.

We are able to see that the two effects in their extremes occur together. These processes are not mutually exclusive in that we can see coincidence of contraction and relaxation. This suggests that at physiological condition, these processes may be co-occurring non-uniformly across the oviducts. Since we are observing the extremes of two effects with a very strong stimulus, we can conclude that the different functions of OA are occurring in parallel with each other. This is a much more reasonable model than OA causes 1 form of activity in opposition to glutamate.

We also show that specific OA receptors, OAMB and OctB2, are responsible for different effects of the oviduct. With these two receptors mutants, we have demonstrated that 2 different effects of OA are mediated by 2 different receptors. The complementary results allow us to determine that OAMB receptor is crucial for a large dilation (relaxation) effect while the OctB2 receptor is essential for lateral oviduct contractions in these isolated reproductive tracts stimulated by OA bath application.

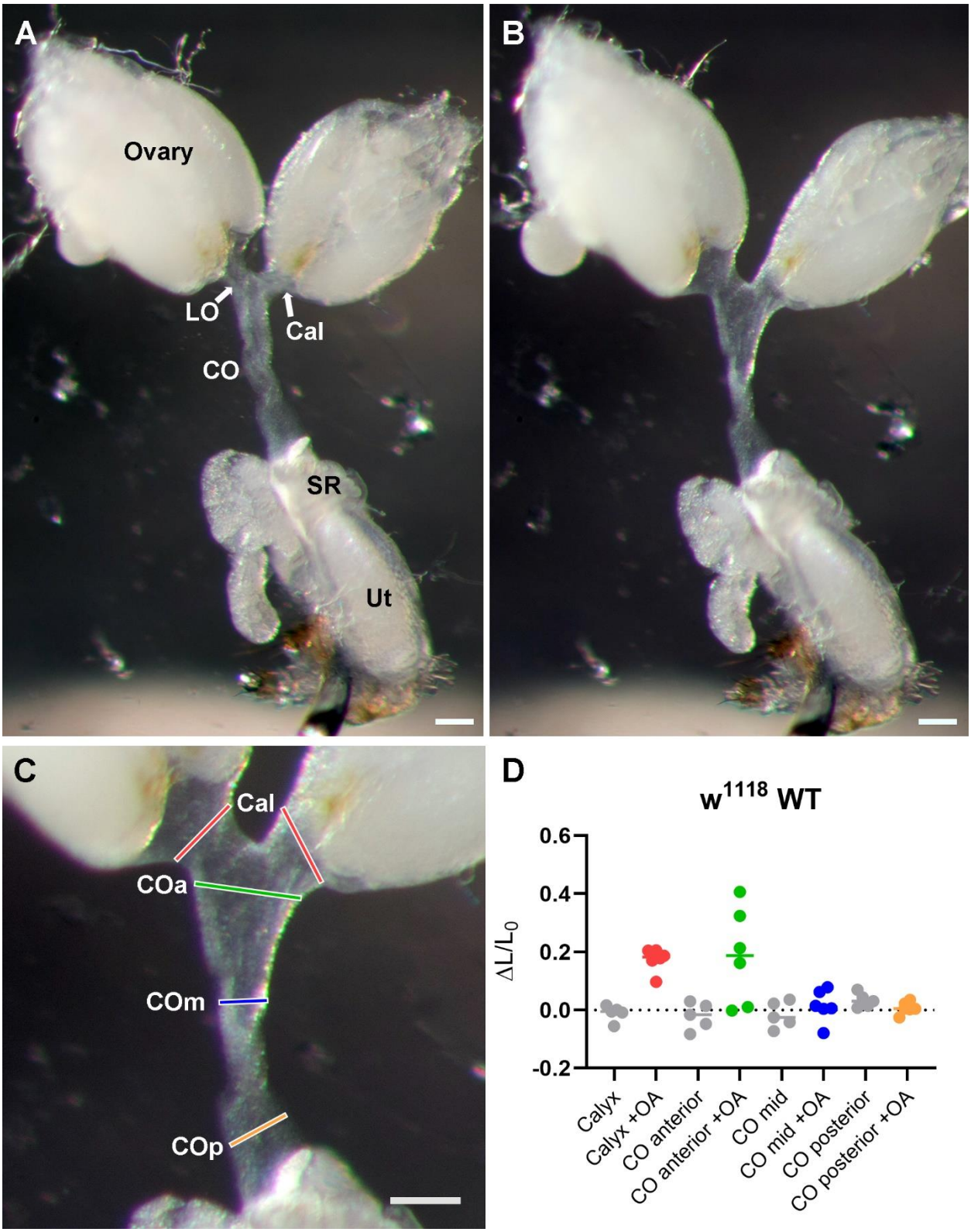
A
Ovary
LO
Cal
CO
SR
Ut
B
C
Cal
COa
COm
COp
D
w1118 WT
0.6
0.4
0.2
0.0
-0.2
ΔL/L0
Calyx
Calyx +OA
CO anterior
CO anterior +OA
CO mid
CO mid +OA
CO posterior
CO posterior +OA

Figure 8. Oviduct Dilation

A. An isolated female reproductive system. (scale bar 100 microns)

B. Same preparation after 9min of incubation in 1mM OA.

C. Enlarged view of oviduct. Each colored bar denotes the anatomical regions measured. These regions include the calyx (Cal) and anterior, mid, and posterior common oviduct.

D. Data plotted for w1118 wild-type. Horizontal lines denote median of group. In grey, each anatomical location prior to OA incubation. Red is relative change in length across the calyx of the lateral oviduct. Green, blue, and orange are the anterior, mid, and posterior common oviduct, respectively. Y-axis represents $\frac{\Delta L}{L0}$, relative change in length at a given location, a proxy for oviduct dilation and luminal expansion. A positive change indicates dilation whereas a negative change indicates contraction. Increases in relative length occurs at the calyx and anterior common oviduct.

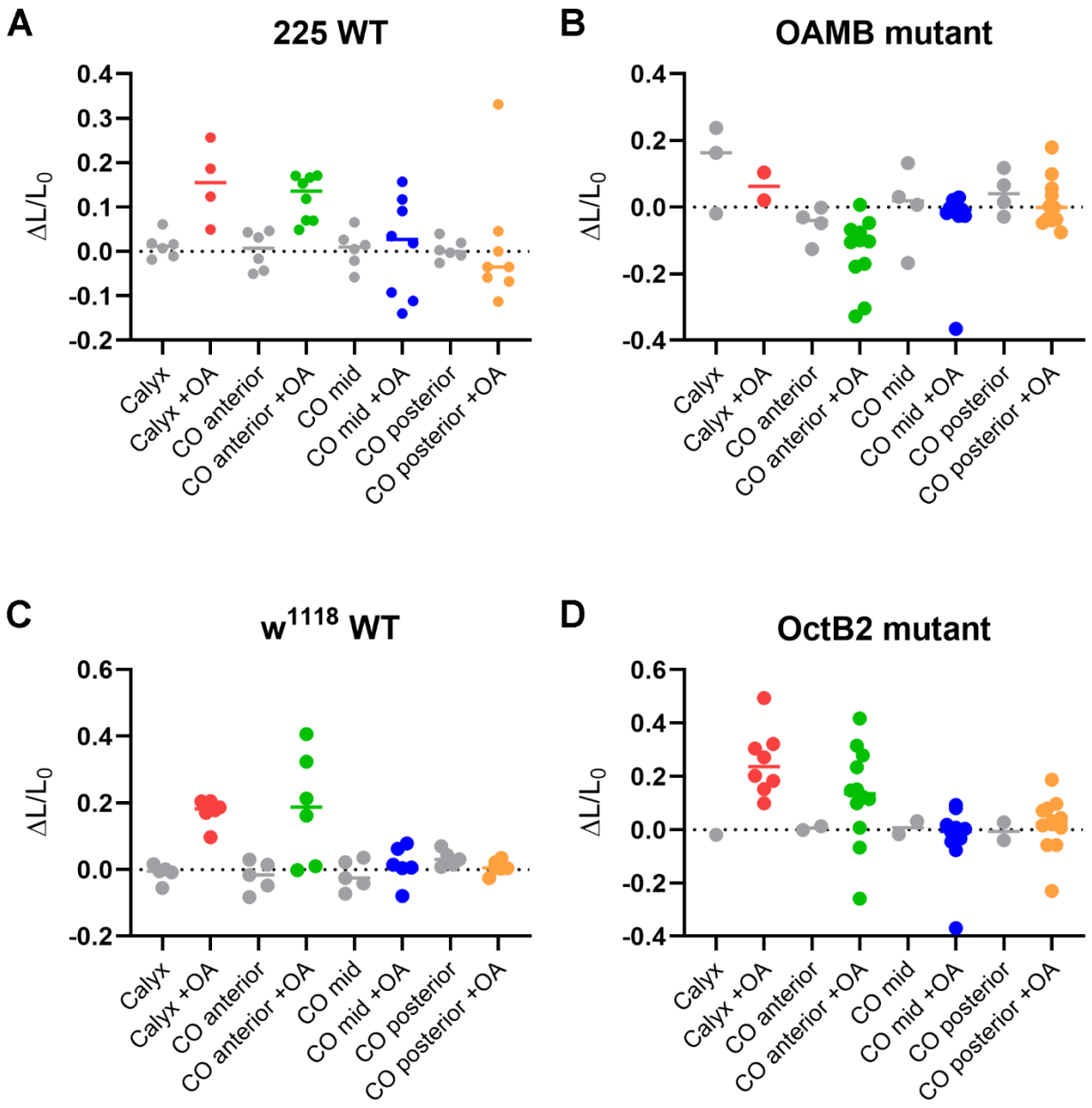

Figure 9. Degree of relaxation at each region of the oviduct for a given genotype.

In grey, vehicle control is added to oviducts and does not produce dilation. In color, OA is added to final concentration of 1mM and causes relaxation at the calyx and anterior common oviduct.

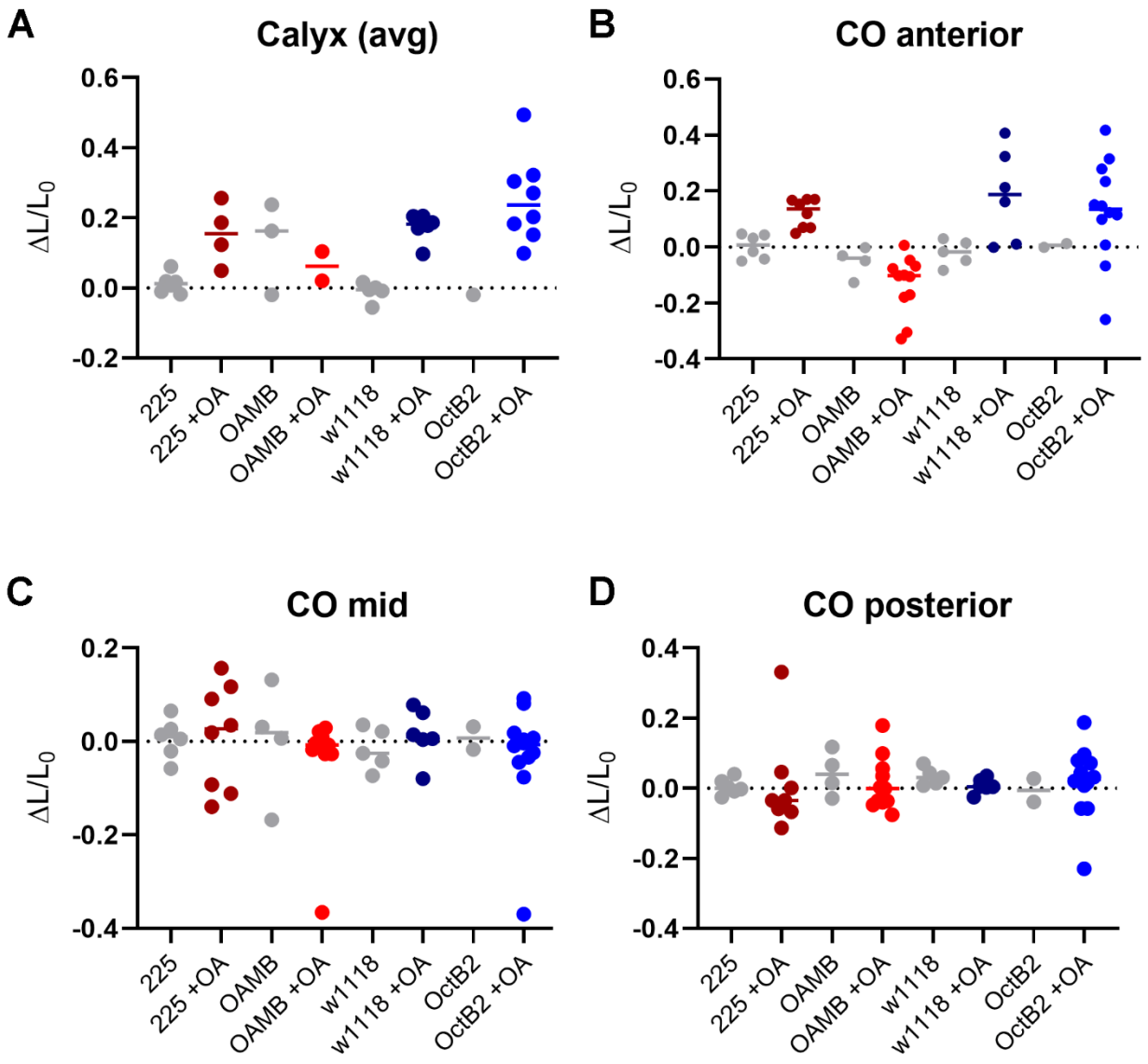

Figure 10. Degree of relaxation compared across genotypes for a given region of the oviduct.

In grey, vehicle control is added and does not produce dilation.

Maroon and red display 225 WT control and OAMB mutant. Navy and blue display w1118 WT control and OctB2 mutant.

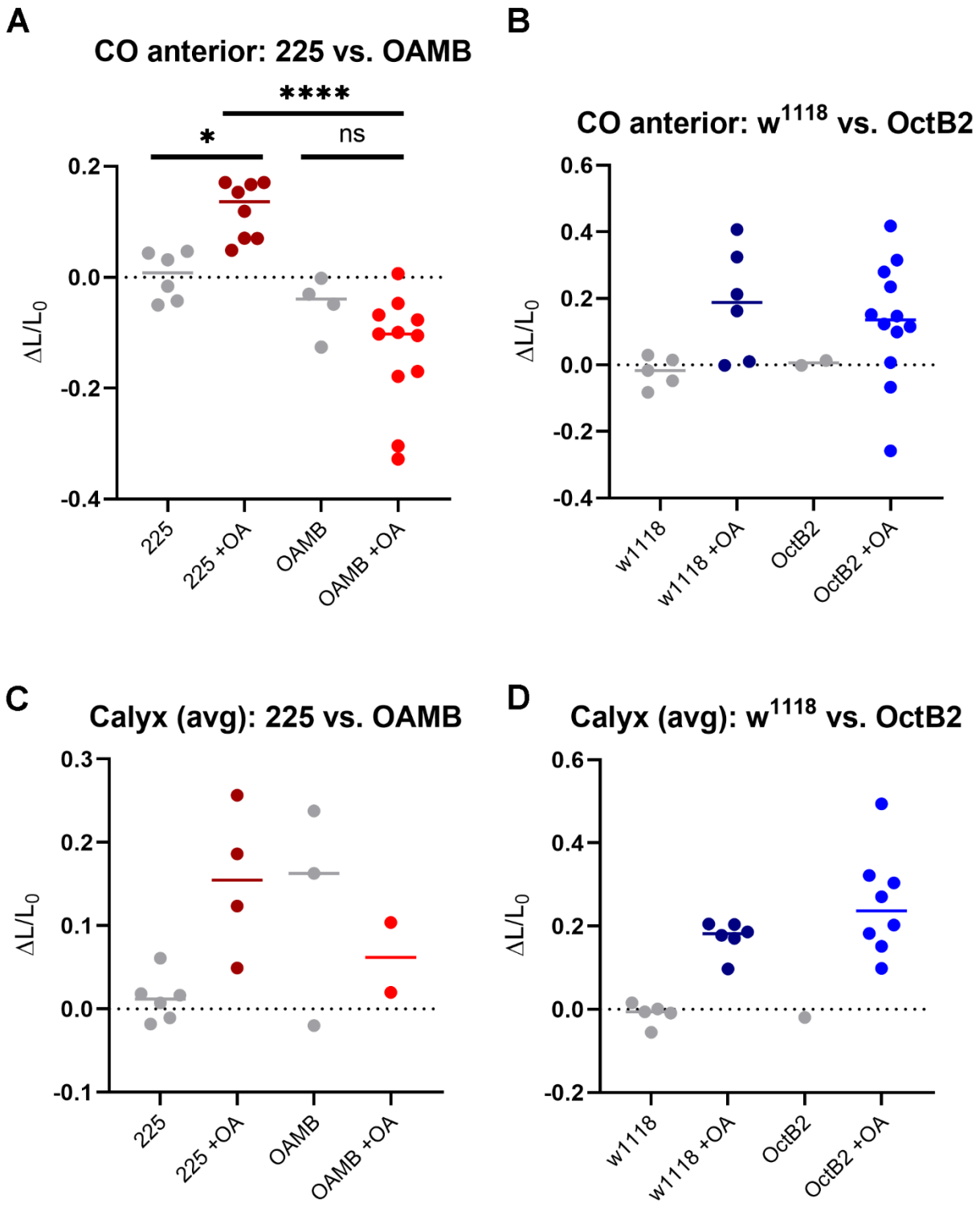

Figure 11. Comparisons between OA receptor mutant and genetically-controlled background.

A. At the anterior common oviduct, 225 WT increases in length with OA (maroon). By contrast, the OAMB mutant does not increase but rather decreases in length (red). (One-way ANOVA with Bonferroni Multiple Comparisons Test, see Appendix)

B. There are no differences between w1118 and OctB2 at the anterior common oviduct.

C. And D. No differences found at the calyx (averaged between 2 sides) for either OAMB and OctB2 and their corresponding WT controls.

Chapter 4

DVMATΔ3 behavioral experiments

Newly generated Δ3 mutants exhibit phenotypes that resemble previous genetic rescue experiments. 4 Δ3 fly lines (F8A, F32A, M23A, and M30A) were chosen to compare to a "wild-type" fly line (F7B) that all came through the CRISPR/Cas9 mutagenesis pipeline.

Although the generated mutants were not outcrossed, the use of a "wild-type" fly line that was generated in the same experiment serves as a fair control genotype. The 4 Δ3 mutants come from 4 different germline mosaic parents. All matched in molecular genotype and phenotype.

I did not out-cross the generated Δ3 mutant to wild-type backgrounds such as Canton-S or w1118. For the purposes of these behavioral experiments, I reasoned that the internal control with F-7B was sufficient for these gross behavioral phenotypes given how closely they resembled the genetic rescue experiments.

Out-crossing will be important in further studies into more complex behaviors.

Key Points

Hypothesis: *DVMATΔ3* trafficking mutation will cause female infertility and lack of egg-laying.

Result: Fertility and average number of eggs laid is significantly decreased, however not zero.

Fertility

Flies were collected under CO2 anesthesia 0–5 d before mating. One virgin female was mated with 4 white1118 males in a vial at room temperature. Twelve days after initial mating, parents were removed and candidates were scored as fertile if the vial contained at least one larva, pupa, or adult.

Egg laying

Five females of the indicated genotype were mated to five white1118 control males in a vial for 3 days. Mated flies were then passed into a new vial each day for 10 d, and the number of eggs laid was counted each day.

The Δ3 mutants have dramatically reduced egg-laying (fecundity) when compared to the internal control. The flies remain fertile since the few eggs laid develop into viable animals. The flies that are able to lay eggs are reproductively fertile, however the regulation and machinery (organs) may be disrupted by the trafficking mutation. The observed infertility is likely due to the lack of egg-laying. Eggs are retained in ovaries still gives rise viable animals.

Larval locomotion assay

Two to three larvae were placed on the food for 30 sec to acclimate and locomotion was scored as the number of 0.4 cm grids crossed over 2 minutes. Their speed was calculated as centimeters per second (cm/s). No significant differences were found between wild-type and Δ3 mutants, just as seen in previously genetic rescue experiments.

Octopaminergic neurons with the VMAT trafficking mutations lack certain functions of ovulation

A work in progress. Once the mutant was created and recombined with *TDC2-GAL4* and *TDC2-LEXA* (which took nearly 1 year), I was able to continue recombination with useful UAS and lexAop lines like channelrhodopin, GCaMP and RCaMP. I was able to test DVMAT trafficking effects on OA neurons' ability to drive lateral oviduct contractions. In this experimental set up, stimulation of the neurons is sufficient to drive lateral oviduct contractions. However, the robustness in response differs between DVMAT WT and Δ3 alleles. While these experiments are not optimized, they are paused due to the world events of 2020.

I was able to identify a gross difference in response to stimulation measured by number of contractions in a given light stimulation epoch. I also observed that maximum number of contractions that can be stimulated is reduced in the mutant. That is, DVMAT WT flies contract more and for longer than *DVMATΔ3* mutants before stopping. WT flies also require less time to recovery following OA depletion with maximum light stimulation. WT flies reliable recover within 30 seconds and 60 seconds whereas Δ3 mutants do not recover to the same degree even after 60 seconds.

<u>Key Points</u>

Hypothesis: *DVMATΔ3* confers infertility and low fecundity due to loss of oviduct contractions.

Results: When stimulated, OA neurons elicit fewer lateral oviduct contractions and take longer time to recover and drive contractions after maximum stimulation.

The mutant fly exhibits an accumulation of eggs in the ovaries. Although the fly is fertile and lays a low number of eggs, the ovaries retain mature follicles. In this experimental paradigm, I used crispr mutagenesis and the binary expression systems in *Drosophila* to create a genotype

homozygous for the delta3 mutation and 2 copies of *TDC2-LEXA*. These recombinants then drive channelrhodopsin in OA neurons in the context of the Δ3 mutation.

Methods and Materials

The posterior end of the abdomen is opened on the ventral side. A ventral approach avoids having to dissect through muscles and organs from dorsal. Furthermore, the neurons of interest are located on the ventral, midline surface of the abdominal ganglion. 2 ventral windows are opened to expose the abdominal ganglion and the female reproductive system. The flies are then placed on the wide-field microscope for imaging for optogenetic stimulation and visualization of movement of female reproductive organs.

The preparation is acclimated to the microscope and is allowed 3-5min of rest. Baseline activity is recorded for 1 minute prior to stimulation. Light is delivered through the objective onto the preparation, either in constant light or pulsed light. The brightness/power of the light output is varied by an LED controller (Thor Labs DC2200).

Flies are stimulated for 30 seconds and contractions are observed before, during, and after the stimulation. Upon illumination, the OA neurons are excited and lateral oviduct contractions ensue. Other organs can be seen to move as well, including ovaries, spermathecae, and the uterus. This experiment leaves the circuit intact, with minimal disruption in dissection.

Preliminary Results

Contractions in wild-type flies have very little latency from light ON to first contraction. Sometimes they have some level of spontaneous activity, however this may also be low level stimulation due to blue light coming from the light source for illumination.
The WT experiment demonstrates that that OA neurons are sufficient to drive contraction of the lateral oviduct, as well as other organs. I and others have shown that OA has multiple effects on the female reproductive system.

Here I am able to demonstrate that when OA neurons are excited by channelrhodopsin, the lateral oviducst (among other organs) contracts similarly to the WT fly. In this experiment, I am able to reliably evoke contractions in *DVMAT∆3* mutants, however there are key differences from WT.

The major difference I observed was that WT flies tend to have more baseline activity than mutants. In the 30second light ON stimulation, WT flies produce 20-30 large lateral oviduct contractions whereas ∆3 mutants produce 7-13 contractions.

The maximum output of the OA neurons can be observed by light stimulation until the oviduct stops contracting. WT flies will contract 25-35 times before stopping after about 70 seconds. In contrast, the ∆3 mutants will max out during the 30 second light stimulation and only produce 7-13 contractions.

I also tested the recovery following maximum stimulation. Following long light ON stimulations where the oviduct stops responding, I varied the next stimulation in time by allowing 30 or 60sec of recovery time.

WT flies are able to recover within the 30 seconds and can respond with contraction when stimulated. These contractions after recovery are fewer in number and longer latency to first contraction. By 60 seconds, the response has reliably recovered, again with fewer number of contractions and longer latency than prior to maximum stimulation dumping OA. In contrast, the ∆3 fly does not recovery within 30 seconds and sometimes during 60 seconds of rest. I have also observed that more time will lead to recovery with more robust of a response. While these experiments are somewhat loosely controlled, an obvious difference between WT and ∆3 is the ability to drive contractions, how many contractions, and how long it takes to recover. These experiments roughly test the amount of OA loaded into vesicles and released and their post-synaptic response, similar to quantal content measured for fast neurotransmission.

Areas for improvement and development

These experiments are somewhat rough and not well controlled. There are several improvements to be made and more refined experiments are already planned. However, due to the COVID-19 pandemic in March 2020, I am not able to complete these experiments.

Issues that need to be addressed include

Low number of experiments

Establish stimulation paradigm

Use of gross motion to quantify oviduct activity

I have plenty of experiments from optimization, however these are hard to compare without the wild-type control. I was able to conduct only a few experiments with fair WT vs Δ3 genotype comparison, but not with a well-developed stimulation paradigm.

This motion is grossly seen by eye and only large lateral oviduct contractions can easily be counted. The ovaries are always full of mature follicles so visualization in the mutant is substantially more difficult. This is best addressed by calcium imaging the muscle as done in bath application experiments. This experiment is much more idealized in that there will be fixed times/durations for stimulation and recovery. Calcium imaging the muscle will also give us more quantitative measurement of oviduct contractions.

Unfortunately, with the pandemic these experiments cannot be done any time soon and will have to wait. These world events have affected everyone's research and practice of medicine. These experiments however are ready to go, so upon return to laboratory research will resume quickly. Current laboratory members and i can also continue these experiments when normal activity resumes.

Nonetheless, I have demonstrated that the *DVMATΔ3* trafficking mutation in the endogenous locus cause low fertility and fecundity. I have also shown that OA neurons that innervate the

female reproductive tract drive contractions. These contractions are still intact in the *DVMAT∆3* trafficking mutant, albeit at less robust of a response.

Future Experiments

Several future experiments are planned and I have created several genotypes that idealize optogenetic tools for investigating these OA circuits.

∆3, TDC2-LEXA ; LEXAOP-ChrR.XXL with *24B-GAL4; UAS-RCaMP1b*

This allows for stimulation OA neurons and reading calcium signal for contractions of the oviduct. This optimized for reading contractions on wide-field fluorescent microscopy.

∆3, TDC2-LEXA; LEXAOP-CS.ChRimson with *OA Receptor-T2A-GAL4; UAS-GCaMP6f*

This allows for stimulation of OA neurons and reading calcium signal in OA receptor-expressing cells. For 5 OA receptors *OAMB, OctB1, 2, 3, and Oct/Tyr*. Optimized for 2-photon microscopy.

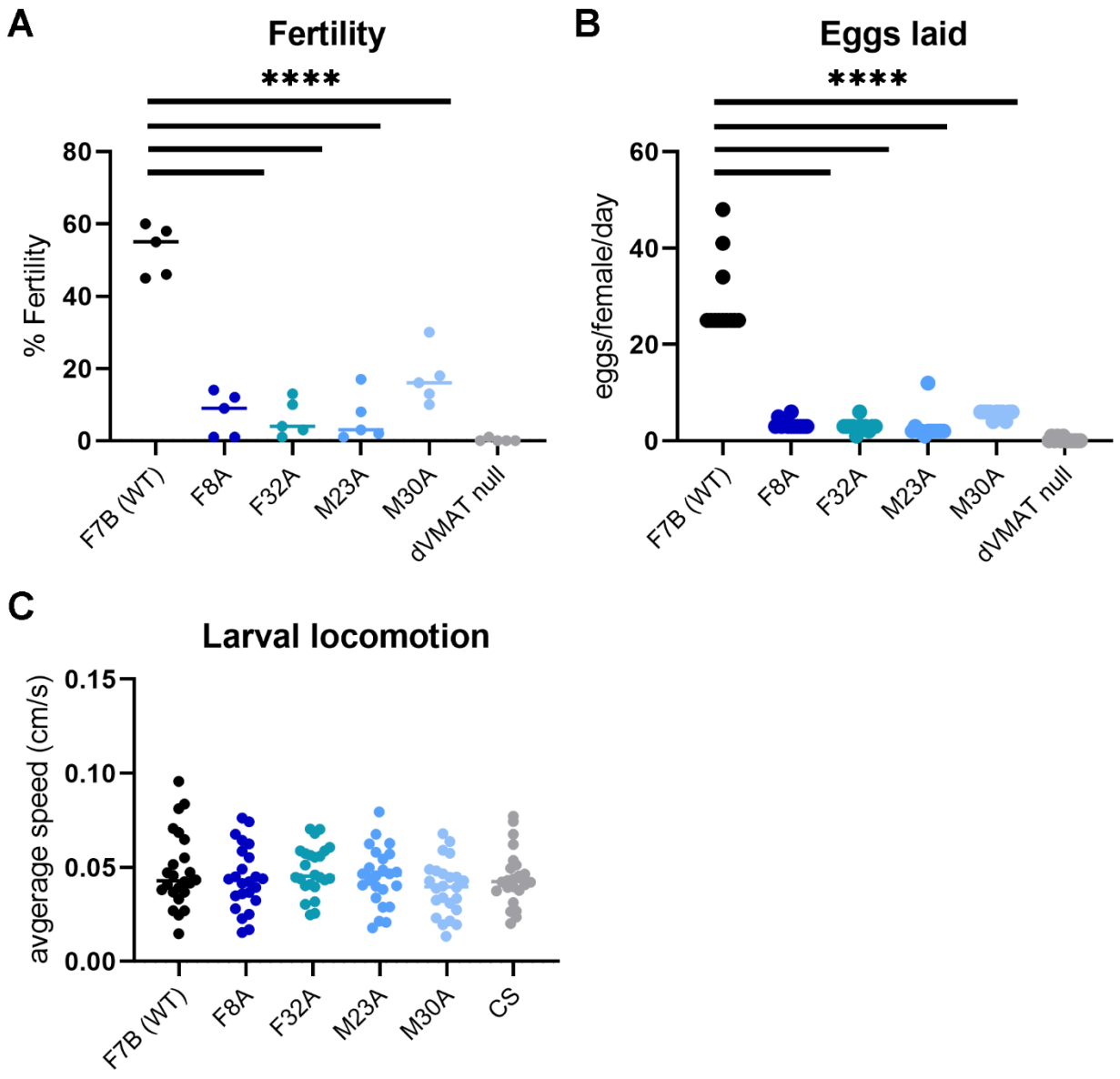

Figure 12. *DVMATΔ3* fertility and egg-laying

A. Fertility of wild-type (F7B) vs 4 *DVMATΔ3* mutant and dVMAT null alleles. Δ3 mutants have significantly decreased fertility compared to wild-type. However, they are not completely infertile like dVMAT null at 0%

B. Eggs laid. Similarly, there is a significantly decrease in number of eggs laid. Δ3 mutants lay significantly fewer eggs than wild-type. However, Δ3 mutants lay more than zero eggs like dVMAT null.

C. Larval locomotion. No significant differences between Δ3 and wild-type controls in average speed of a 3rd instar larval movement.

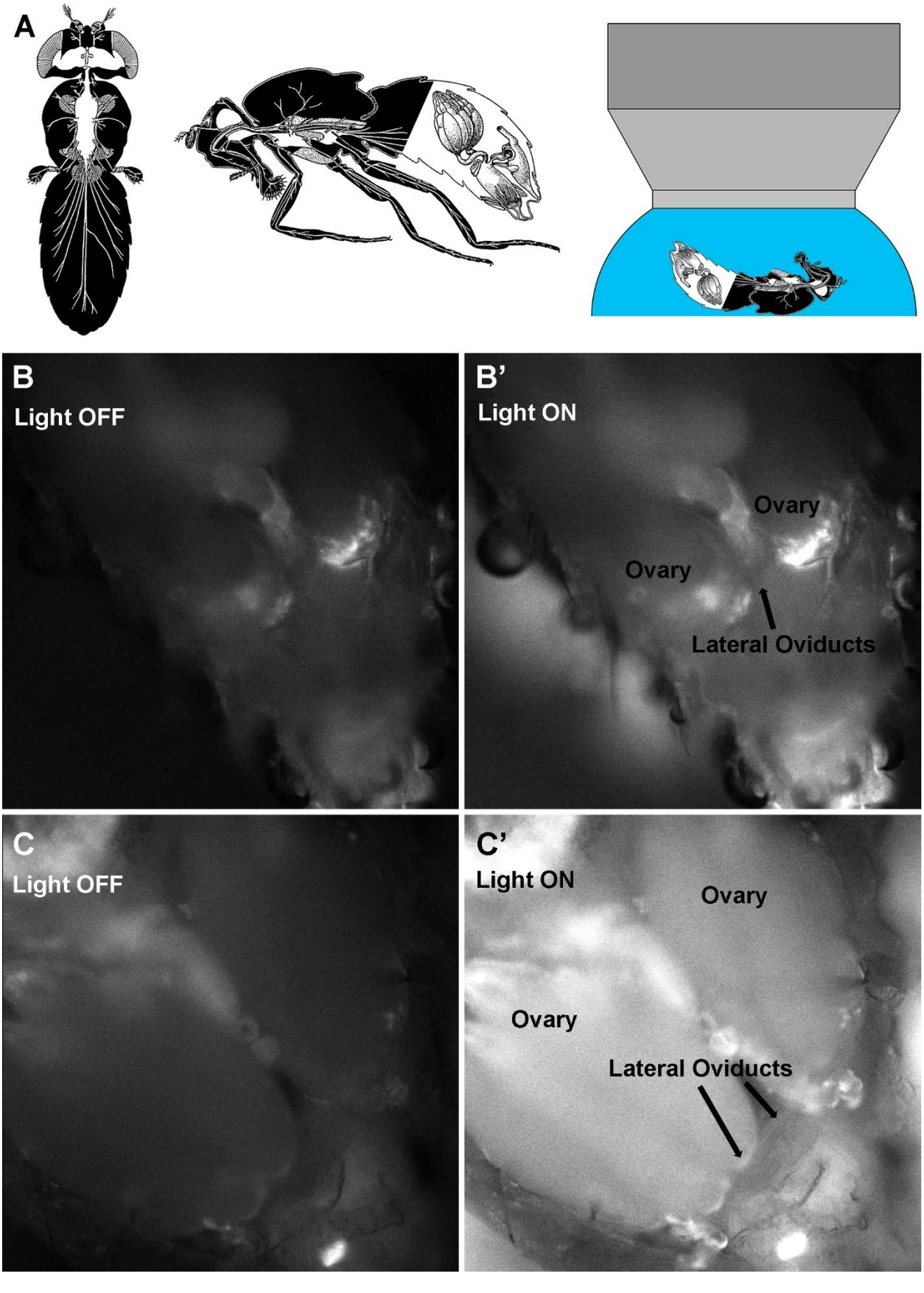
A
B
Light OFF
B'
Light ON
Ovary
Ovary
Lateral Oviducts
C
Light OFF
C'
Light ON
Ovary
Ovary
Lateral Oviducts

Figure 13. TDC2 ChR2 experiments

Optogenetic stimulation of OA neurons elicits lateral oviduct contractions.

A. A cartoon of both ventral and sagittal views of the *Drosophila* nervous system and reproductive organs. Right – Schematic depicting *Drosophila* body adhered to slide surface and ventral side imaged in HL3.1 media.

B. And B'. Wildtype

C. And C'. *DVMAT∆3*

Conclusions and Closing Remarks

I am able to prove my initial hypothesis is wrong by demonstrating that the lateral oviducts contract even in the mutant. A small amount of DVMAT persists on SVs and likely loads a small amount of OA. In my experiment, the maximum stimulation of the neurons may dump all of the OA out and cause contractions. It is possible that at physiological conditions, the amount of OA loaded into SVs is not sufficient to drive contractions.

These experiments demonstrate that this OA signaling pathway is dependent on release from SVs. While the VMAT is distributed away from SVs and towards LDCVs, I see a decrease in lateral oviduct contraction number and longer latency. This indicates that the signaling process from LO contractions is more dependent on SVs than LDCVs. Since there is a decrease in activity that corresponds to decrease DVMAT on SVs, it is more likely to be related to this mode of release. Since VMAT on LDCVs increases with mutation, there is reasonably more release from this vesicle pool. If the lateral oviduct contractions were more LDCV release dependent, I would expect an increase in response in the mutant.

Another explanation of why contractions persist is that the intense stimulation of neurons is dumping all vesicles, both SVs and LDCVs. Even if this is the case, the direction of response change follows the change in VMAT on SVs.

It stands to reason that decreased LO response is a function of decreased OA loaded and released from SVs. In some ways, this may represent quantal content being altered by transporter protein localization. Usually, quantal content refers to the amount of neurotransmitter in a single vesicle, which for fast neurotransmitters is normally measured by the amplitude of change in miniEPSPs. However, this is only really possible to measure for neurotransmitters with ionotropic receptors. While the OA neurons and oviduct muscle are not a typical neuromuscular junction, I

at least see postsynaptic responses that seem to scale with a known vesicular transporter redistribution.

Other explanations of why eggs do not pass even with LO contractions intact may be unrelated to LO contractions all together. It is possible that the defect in ovulation occurs higher up in the female reproductive system (i.e. the ovary and calyx). The expulsion of the egg from ovary into the oviduct likely requires concerted activity of the organs and potentially the neurons.

The eggs may be stuck in the ovary because of the following possibilities

- the ovary contractions are more affected by the mutation
- follicle rupture is heavily dependent SV release
- loss of oviduct relaxation to accommodate the egg
- the concerted activity of the group of OA neurons is disrupted

Loss of any of these functions may indicate that a particular OA neuron and target organ is dependent on SV release.

Suppose ovulation had significant amount of local regulation of activity. OA release onto these local neurons, muscles, and tissues may trigger metabolic changes in target cells that then bias the activity from not ovulating to increased movement in organs. This would imply that OA is able to switch the state the reproductive system is in. Once OA has had its metabolic effects on post-synaptic cells, the local system may now be sufficient to drive ovulation without additional OA input from the abdominal ganglion. This does not seem to be the case since there is little enduring and self-perpetuating activity following stimulation of OA neurons.

Alternatively, ovulation may be regulated directly by the neurons, where OA has particular effects on organs, but any coordinated activity is orchestrated by higher order neurons such as a central pattern generator or by intrinsic properties of the OA neurons as a functioning group. In this case

OA signaling is top-down regulation of ovulation, where OA neurons themselves dictate their own pattern or are governed by a central pattern generator above it.

These new genetic reagents I have created and experiments demonstrate that OA signaling in the female reproductive system has a variety of functions. These functions are likely regulated by the specific neuronal innervation and receptor expression in particular cell types for a given organ. These neurons are sufficient to drive contractions of certain organs, giving them an NMJ-like quality. The experimental approach of mutagenesis to alter VMAT trafficking by CRISPR/Cas9 and subsequent recombination with transgenes have created a very powerful platform to study OA signaling. I have also shown that egg retention in the ovaries not solely due to lack of contraction and these two are separable events in ovulation. This suggests that coordinated activity of the reproductive organs likely requires normal release of OA from SVs. In doing so, I have been able to demonstrate that the amount of VMAT on SVs affects the amount of response from post-synaptic muscles, a potentially quantal content of OA in a SV. Further studies can further quantify alterations in activity by the trafficking mutation and elucidate which OA pathways are dependent on SV and LDCV release.

This work represents efforts to understand monoamine neurotransmitter release modes in the context of a model circuit. The biological processes affected neurotransmitter release mode in complex behaviors and circuits remain mysterious. Having mapped and defined function of the female reproductive system, this model circuit is the ideal platform to investigate effects of different modes of monoamine neurotransmitter release.

Appendix

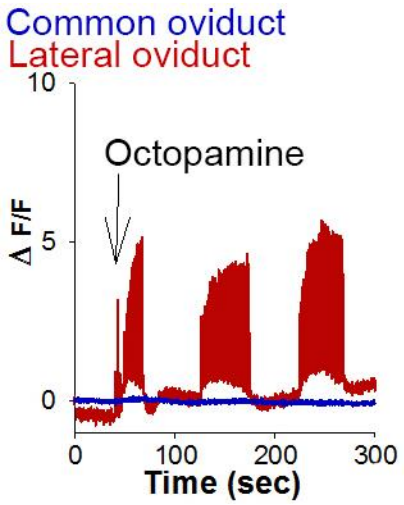

A1. OA stimulates lateral oviduct contractions

Example from Sonali Deshpande's work on oviduct contractions. Y-axis is change in fluorescence signal from GCaMP6m, a fluorescent calcium indicator. An increase in fluorescence reflects increases in calcium in oviduct muscle during contraction. In red is activity in the lateral oviduct and in blue is the common oviduct.

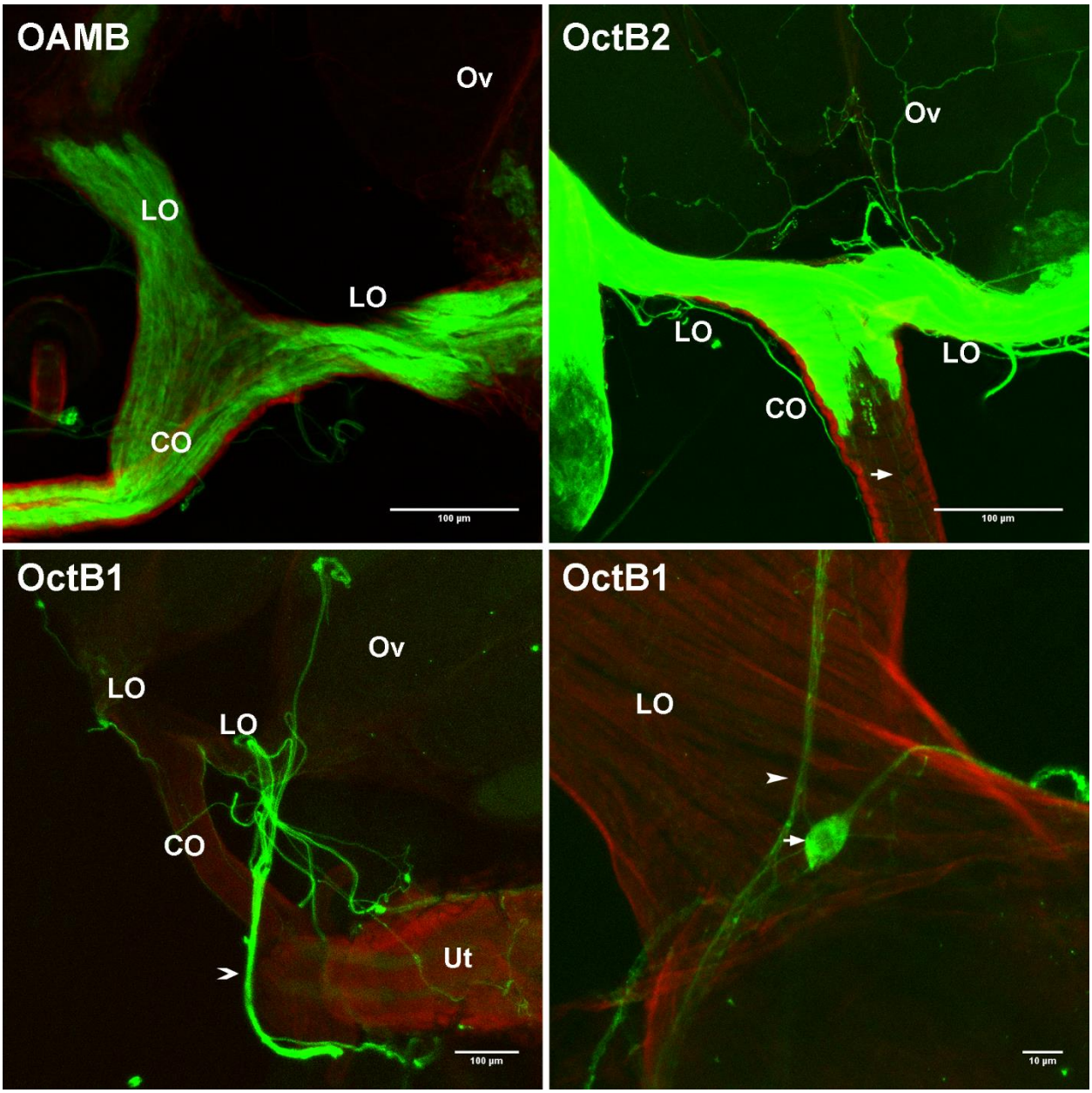

A2. OA receptor expression in the female reproductive tract

OAMB – green is OAMB-T2A-GAL4, red phalloidin. OAMB is expressed in epithelia of the lumen throughout the lateral and common oviducts.

OctB2 – OctB2 is expressed in epithelia of only the lateral oviducts and fine neuron-like processes in the ovaries and common oviduct.

OctB1 – OctB1 is expressed in neurons external to the muscles of the reproductive tract.

Media uploads

OA dilation example

AVI video file: OA dilation example.avi

Video demonstrating gradual dilation of the oviduct. Simultaneously, bursts of contractions occur. 10 minute experiment condense to 1 min video (10 fps).

Wild-type and *DVMATΔ3* optogenetic experiments

AVI video files: WT example 20200310.avi DVMATD3 example 320200228.avi

Video depicts a ventral view of the abdominal organs visualized by wild-field microscopy. When the LED light comes on, both wild-type and *DVMATΔ3* genotypes respond with contractions of the lateral oviduct. These contractions pull the ovaries towards each other.

TDC2 Multi-Color Flp-Out – example images

TIFF image file: MCFO matrix.tif

A large poster with additional example images of TDC2 MCFO preparations that illustrate OA neurons innervating distinct regions of the female reproductive system.

TDC2 MCFO cells counted

Abbreviated names	Number of times counted (in 46 animals)
Ov	6
Cal	8
LO	4
LO+COa	4
Cop+Uta+SR	6
Utp	11
SpA	10
SpB	5
Pa	3

Statistics

Fertility

ANOVA summary	
F	52.47
P value	<0.0001
P value summary	****
Significant diff. among means (P < 0.05)?	Yes
R squared	0.9162

Brown-Forsythe test			
F (DFn	DFd)	1.039 (5	24)
P value	0.4178		
P value summary	ns		
Are SDs significantly different (P < 0.05)?	No		

Bartlett's test	
Bartlett's statistic (corrected)	16.24
P value	0.0062
P value summary	**
Are SDs significantly different (P < 0.05)?	Yes

ANOVA table	SS	DF	MS	F (DFn	DFd)	P value
Treatment (between columns)	9331	5	1866	F (5	24) = 52.47	P<0.0001
Residual (within columns)	853.6	24	35.57			
Total	10185	29				

Data summary	
Number of treatments (columns)	6
Number of values (total)	30

Bonferroni's multiple comparisons test	Mean Diff.	95.00% CI of diff.	Significant?	Summary	Adjusted P Value
F7B (WT) vs. F8A	45.4	34.85 to 55.95	Yes	****	<0.0001
F7B (WT) vs. F32A	46.6	36.05 to 57.15	Yes	****	<0.0001
F7B (WT) vs. M23A	46.6	36.05 to 57.15	Yes	****	<0.0001
F7B (WT) vs. M30A	35.4	24.85 to 45.95	Yes	****	<0.0001
F7B (WT) vs. dVMAT null	52.6	42.05 to 63.15	Yes	****	<0.0001

Test details	Mean 1	Mean 2	Mean Diff.	SE of diff.	n1	n2	t	DF
F7B (WT) vs. F8A	52.8	7.4	45.4	3.772	5	5	12.04	24
F7B (WT) vs. F32A	52.8	6.2	46.6	3.772	5	5	12.35	24
F7B (WT) vs. M23A	52.8	6.2	46.6	3.772	5	5	12.35	24
F7B (WT) vs. M30A	52.8	17.4	35.4	3.772	5	5	9.385	24
F7B (WT) vs. dVMAT null	52.8	0.2	52.6	3.772	5	5	13.95	24

Number of families	1
Number of comparisons per family	5
Alpha	0.05

Descriptive Statistics	F7B (WT)	F8A	F32A	M23A	M30A	dVMAT null
Number of values	5	5	5	5	5	5
Minimum	45	1	1	1	10	0
25% Percentile	45.5	1	2	1.5	11.5	0
Median	55	9	4	3	16	0
75% Percentile	59	13	11.5	12.5	24	0.5
Maximum	60	14	13	17	30	1
Mean	52.8	7.4	6.2	6.2	17.4	0.2
Std. Deviation	6.907	6.107	5.07	6.611	7.668	0.4472
Std. Error of Mean	3.089	2.731	2.267	2.956	3.429	0.2
Lower 95% CI	44.22	-0.1833	-0.09464	-2.008	7.879	-0.3553
Upper 95% CI	61.38	14.98	12.49	14.41	26.92	0.7553

Eggs Laid

ANOVA summary	
F	112.2
P value	<0.0001
P value summary	****
Significant diff. among means (P < 0.05)?	Yes
R squared	0.8962

Brown-Forsythe test			
F (DFn	DFd)	2.044 (5	65)
P value	0.084		
P value summary	ns		
Are SDs significantly different (P < 0.05)?	No		

Bartlett's test	
Bartlett's statistic (corrected)	109.8
P value	<0.0001
P value summary	****
Are SDs significantly different (P < 0.05)?	Yes

ANOVA table	SS	DF	MS	F (DFn	DFd)	P value
Treatment (between columns)	6915	5	1383	F (5	65) = 112.2	P<0.0001
Residual (within columns)	801.2	65	12.33			
Total	7717	70				

Data summary	
Number of treatments (columns)	6
Number of values (total)	71

Bonferroni's multiple comparisons test	Mean Diff.	95.00% CI of diff.	Significant?	Summary	Adjusted P Value
F7B (WT) vs. F8A	25.54	21.74 to 29.35	Yes	****	<0.0001
F7B (WT) vs. F32A	26	22.20 to 29.80	Yes	****	<0.0001
F7B (WT) vs. M23A	26.17	22.36 to 29.97	Yes	****	<0.0001
F7B (WT) vs. M30A	23.36	19.47 to 27.25	Yes	****	<0.0001
F7B (WT) vs. dVMAT null	28.75	24.95 to 32.55	Yes	****	<0.0001

Test details	Mean 1	Mean 2	Mean Diff.	SE of diff.	n1	n2	t	DF
F7B (WT) vs. F8A	29	3.458	25.54	1.433	12	12	17.82	65
F7B (WT) vs. F32A	29	3	26	1.433	12	12	18.14	65
F7B (WT) vs. M23A	29	2.833	26.17	1.433	12	12	18.26	65
F7B (WT) vs. M30A	29	5.636	23.36	1.466	12	11	15.94	65
F7B (WT) vs. dVMAT null	29	0.25	28.75	1.433	12	12	20.06	65

Number of families	1
Number of comparisons per family	5
Alpha	0.05

Descriptive Statistics	F7B (WT)	F8A	F32A	M23A	M30A	dVMAT null
Number of values	12	12	12	12	11	12
Minimum	25	3	1	1	4	0
25% Percentile	25	3	3	2	6	0
Median	25	3	3	2	6	0
75% Percentile	31.75	3.375	3	2	6	0.75
Maximum	48	6	6	12	6	1
Mean	29	3.458	3	2.833	5.636	0.25
Std. Deviation	7.828	0.9876	1.128	2.918	0.809	0.4523
Std. Error of Mean	2.26	0.2851	0.3257	0.8424	0.2439	0.1306
Lower 95% CI	24.03	2.831	2.283	0.9793	5.093	-0.03736
Upper 95% CI	33.97	4.086	3.717	4.687	6.18	0.5374

Larval Locomotion

ANOVA summary	
F	1.086
P value	0.3708
P value summary	ns
Significant diff. among means (P < 0.05)?	No
R squared	0.03787

Brown-Forsythe test				
F (DFn	DFd)	0.5892	(5	138)
P value	0.7083			
P value summary	ns			
Are SDs significantly different (P < 0.05)?	No			

Bartlett's test	
Bartlett's statistic (corrected)	5.299
P value	0.3805
P value summary	ns
Are SDs significantly different (P < 0.05)?	No

ANOVA table	SS	DF	MS	F (DFn	DFd)	P value
Treatment (between columns)	0.001378	5	0.0002757	F (5	138) = 1.086	P=0.3708
Residual (within columns)	0.03503	138	0.0002538			
Total	0.0364	143				

Data summary	
Number of treatments (columns)	6
Number of values (total)	144

Bonferroni's multiple comparisons test	Mean Diff.	95.00% CI of diff.	Significant?	Summary	Adjusted P Value
F7B (WT) vs. CS	0.003856	-0.008156 to 0.01587	No	ns	>0.9999
F7B (WT) vs. F8A	0.004174	-0.007839 to 0.01619	No	ns	>0.9999
F7B (WT) vs. F32A	-0.0002547	-0.01227 to 0.01176	No	ns	>0.9999
F7B (WT) vs. M23A	0.00322	-0.008792 to 0.01523	No	ns	>0.9999
F7B (WT) vs. M30A	0.009031	-0.002982 to 0.02104	No	ns	0.2579

Test details	Mean 1	Mean 2	Mean Diff.	SE of diff.	n1	n2	t	DF
F7B (WT) vs. CS	0.0482	0.04435	0.003856	0.004599	24	24	0.8384	138
F7B (WT) vs. F8A	0.0482	0.04403	0.004174	0.004599	24	24	0.9075	138
F7B (WT) vs. F32A	0.0482	0.04846	-0.0002547	0.004599	24	24	0.05537	138
F7B (WT) vs. M23A	0.0482	0.04498	0.00322	0.004599	24	24	0.7003	138
F7B (WT) vs. M30A	0.0482	0.03917	0.009031	0.004599	24	24	1.964	138

Number of families	1
Number of comparisons per family	5
Alpha	0.05

	CS	F7B (WT)	F8A	F32A	M23A	M30A
Number of values	24	24	24	24	24	24
Minimum	0.02014	0.01482	0.01531	0.02472	0.01788	0.01329
25% Percentile	0.03755	0.03684	0.03302	0.04049	0.03486	0.02827
Median	0.04242	0.04286	0.04313	0.04538	0.04598	0.03966
75% Percentile	0.05082	0.06239	0.05778	0.05839	0.05641	0.04776
Maximum	0.07711	0.09577	0.07621	0.07037	0.07951	0.06791
Mean	0.04435	0.0482	0.04403	0.04846	0.04498	0.03917
Std. Deviation	0.01472	0.02007	0.01696	0.01308	0.01536	0.01445
Std. Error of Mean	0.003004	0.004098	0.003462	0.002671	0.003134	0.002949
Lower 95% CI	0.03813	0.03973	0.03687	0.04293	0.0385	0.03307
Upper 95% CI	0.05056	0.05668	0.05119	0.05398	0.05147	0.04527

Common Oviduct anterior – dilation

225 vs OAMB

ANOVA summary	
F	17.83
P value	<0.0001
P value summary	****
Significant diff. among means (P < 0.05)?	Yes
R squared	0.6815

Brown-Forsythe test			
F (DFn	DFd)	0.8811 (3	25)
P value	0.4643		
P value summary	ns		
Are SDs significantly different (P < 0.05)?	No		

Bartlett's test	
Bartlett's statistic (corrected)	6.34
P value	0.0962
P value summary	ns
Are SDs significantly different (P < 0.05)?	No

ANOVA table	SS	DF	MS	F (DFn	DFd)	P value
Treatment (between columns)	0.3089	3	0.103	F (3	25) = 17.83	P<0.0001
Residual (within columns)	0.1443	25	0.005774			
Total	0.4532	28				

Data summary	
Number of treatments (columns)	4
Number of values (total)	29

Bonferroni's multiple comparisons test	Mean Diff.	95.00% CI of diff.	Significant?	Summary	Adjusted P Value
225 vs. 225 +OA	**-0.1192**	**-0.2367 to -0.001590**	**Yes**	*****	**0.0456**
225 vs. OAMB	0.05381	-0.08671 to 0.1943	No	ns	>0.9999
225 vs. OAMB +OA	0.136	0.02554 to 0.2465	Yes	**	0.0099
225 +OA vs. OAMB	0.173	0.03966 to 0.3063	Yes	**	0.0061
225 +OA vs. OAMB +OA	**0.2552**	**0.1540 to 0.3563**	**Yes**	********	**<0.0001**
OAMB vs. OAMB +OA	**0.08222**	**-0.04489 to 0.2093**	**No**	**ns**	**0.4543**

Test details	Mean 1	Mean 2	Mean Diff.	SE of diff.	n1	n2	t	DF
225 vs. 225 +OA	0.001875	0.121	-0.1192	0.04104	6	8	2.904	25
225 vs. OAMB	0.001875	0.05193	-0.05381	0.04905	6	4	1.097	25
225 vs. OAMB +OA	0.001875	-0.1341	0.136	0.03856	6	11	3.527	25
225 +OA vs. OAMB	0.121	0.05193	0.173	0.04653	8	4	3.717	25
225 +OA vs. OAMB +OA	0.121	-0.1341	0.2552	0.03531	8	11	7.227	25
OAMB vs. OAMB +OA	-0.05193	-0.1341	0.08222	0.04437	4	11	1.853	25

Number of families	1
Number of comparisons per family	6
Alpha	0.05

	225	225 +OA	OAMB	OAMB +OA
Number of values	6	8	4	11
Minimum	-0.05012	0.04857	-0.1264	-0.3279
25% Percentile	-0.04481	0.06971	-0.107	-0.1789
Median	0.007478	0.136	-0.03975	-0.1027
75% Percentile	0.0439	0.1695	0.009068	-0.06826
Maximum	0.04638	0.1708	-0.00186	0.006412
Mean	0.001875	0.121	-0.05193	-0.1341
Std. Deviation	0.04384	0.05144	0.05326	0.1038
Std. Error of Mean	0.0179	0.01819	0.02663	0.03129
Lower 95% CI	-0.04414	0.07803	-0.1367	-0.2039
Upper 95% CI	0.04789	0.164	0.03282	-0.06443

Common Oviduct anterior dilation

W1118 vs OctB2

ANOVA summary	
F	2.027
P value	0.1409
P value summary	ns
Significant diff. among means (P < 0.05)?	No
R squared	0.2246

Brown-Forsythe test			
F (DFn	DFd)	1.816 (3	21)
P value	0.1752		
P value summary	ns		
Are SDs significantly different (P < 0.05)?	No		

Bartlett's test	
Bartlett's statistic (corrected)	
P value	
P value summary	
Are SDs significantly different (P < 0.05)?	

ANOVA table	SS	DF	MS	F (DFn	DFd)	P value
Treatment (between columns)	0.145	3	0.04833	F (3	21) = 2.027	P=0.1409
Residual (within columns)	0.5006	21	0.02384			
Total	0.6456	24				

Data summary	
Number of treatments (columns)	4
Number of values (total)	25

Bonferroni's multiple comparisons test	Mean Diff.	95.00% CI of diff.	Significant?	Summary	Adjusted P Value
w1118 vs. w1118 +OA	-0.2062	-0.4784 to 0.06608	No	ns	0.2323
w1118 vs. OctB2	-0.0265	-0.4027 to 0.3497	No	ns	>0.9999
w1118 vs. OctB2 +OA	-0.1507	-0.3900 to 0.08862	No	ns	0.4853
w1118 +OA vs. OctB2	0.1797	-0.1874 to 0.5468	No	ns	>0.9999
w1118 +OA vs. OctB2 +OA	0.05547	-0.1693 to 0.2803	No	ns	>0.9999
OctB2 vs. OctB2 +OA	-0.1242	-0.4676 to 0.2192	No	ns	>0.9999

Test details	Mean 1	Mean 2	Mean Diff.	SE of diff.	n1	n2	t	DF
w1118 vs. w1118 +OA	-0.0206	0.1856	-0.2062	0.09349	5	6	2.205	21
w1118 vs. OctB2	-0.0206	0.005896	-0.0265	0.1292	5	2	0.2051	21
w1118 vs. OctB2 +OA	-0.0206	0.1301	-0.1507	0.08219	5	12	1.834	21
w1118 +OA vs. OctB2	0.1856	0.005896	0.1797	0.1261	6	2	1.425	21
w1118 +OA vs. OctB2 +OA	0.1856	0.1301	0.05547	0.0772	6	12	0.7185	21
OctB2 vs. OctB2 +OA	0.005896	0.1301	-0.1242	0.1179	2	12	1.053	21
Number of families	1							
Number of comparisons per family	6							
Alpha	0.05							

	w1118	w1118 +OA	OctB2	OctB2 +OA
Number of values	5	6	2	12
Minimum	-0.08284	-0.00155	-0.00135	-0.2586
25% Percentile	-0.06523	0.007168	-0.00135	0.0298
Median	-0.01682	0.1873	0.005896	0.1347
75% Percentile	0.02214	0.3445	0.01314	0.2681
Maximum	0.02962	0.4065	0.01314	0.4178
Mean	-0.0206	0.1856	0.005896	0.1301
Std. Deviation	0.04578	0.1643	0.01025	0.1802
Std. Error of Mean	0.02047	0.06709	0.007246	0.05201
Lower 95% CI	-0.07744	0.01312	-0.08617	0.01563
Upper 95% CI	0.03624	0.358	0.09797	0.2446

Bibliography

1. Nirenberg, M.J., et al., *The vesicular monoamine transporter 2 is present in small synaptic vesicles and preferentially localizes to large dense core vesicles in rat solitary tract nuclei.* (0027-8424 (Print)).
2. Nirenberg, M.J., et al., *Ultrastructural localization of the vesicular monoamine transporter-2 in midbrain dopaminergic neurons: potential sites for somatodendritic storage and release of dopamine.* (0270-6474 (Print)).
3. Greer, C.L., et al., *A splice variant of the Drosophila vesicular monoamine transporter contains a conserved trafficking domain and functions in the storage of dopamine, serotonin, and octopamine.* Journal of Neurobiology, 2005. **64**(3): p. 239-258.
4. Grygoruk, A., et al., *The Redistribution of Drosophila Vesicular Monoamine Transporter Mutants from Synaptic Vesicles to Large Dense-Core Vesicles Impairs Amine-Dependent Behaviors.* Journal of Neuroscience, 2014.
5. Simon, A.F., et al., *Drosophila vesicular monoamine transporter mutants can adapt to reduced or eliminated vesicular stores of dopamine and serotonin.* Genetics, 2009. **181**(2): p. 525-541.
6. Gratz, S.J., et al., *CRISPR-Cas9 Genome Editing in Drosophila.* (1934-3647 (Electronic)).
7. Yang, L., et al., *Optimization of scarless human stem cell genome editing.* (1362-4962 (Electronic)).
8. Monastirioti, M., *Distinct octopamine cell population residing in the CNS abdominal ganglion controls ovulation in Drosophila melanogaster.* Developmental biology, 2003. **264**(1): p. 38-49.

9. Cole, S.H., et al., *Two functional but noncomplementing Drosophila tyrosine decarboxylase genes: Distinct roles for neural tyramine and octopamine in female fertility.* Journal of Biological Chemistry, 2005. **280**(15): p. 14948-14955.

10. Nern, A., B.D. Pfeiffer, and G.M. Rubin, *Optimized tools for multicolor stochastic labeling reveal diverse stereotyped cell arrangements in the fly visual system.* Proceedings of the National Academy of Sciences, 2015. **112**(22): p. E2967.

11. Monastirioti, M., *Biogenic amine systems in the fruit fly Drosophila melanogaster - Monastirioti - 1999 - Microscopy Research and Technique - Wiley Online Library.* 1999. **121**(October 1998): p. 106-121.

12. Rodríguez-Valentín, R., et al., *Oviduct contraction in Drosophila is modulated by a neural network that is both, octopaminergic and glutamatergic.* Journal of Cellular Physiology, 2006. **209**(1): p. 183-198.

13. Deady, L.D. and J. Sun, *A Follicle Rupture Assay Reveals an Essential Role for Follicular Adrenergic Signaling in Drosophila Ovulation.* PLOS Genetics, 2015. **11**(10): p. e1005604-e1005604.

14. Heifetz, Y., et al., *Mating regulates neuromodulator ensembles at nerve termini innervating the drosophila reproductive tract.* Current Biology, 2014. **24**(7): p. 731-737.

15. Middleton, C.A., et al., *Neuromuscular organization and aminergic modulation of contractions in the Drosophila ovary.* BMC Biology, 2006. **4**(1): p. 17-17.

16. Lee, H.G., et al., *Octopamine receptor OAMB is required for ovulation in Drosophila melanogaster.* Developmental Biology, 2003. **264**(1): p. 179-190.

17. Lee, H.-G.G., S. Rohila, and K.-A.A. Han, *The octopamine receptor OAMB mediates ovulation via Ca2+/calmodulin-dependent protein kinase II in the Drosophila oviduct epithelium.* PLoS ONE, 2009. **4**(3): p. e4716-e4716.

18. Li, Y., et al., *THE OCTOPAMINE RECEPTOR octß2R IS ESSENTIAL FOR OVULATION AND FERTILIZATION IN THE FRUIT FLY <i>Drosophila*

melanogaster. Archives of Insect Biochemistry and Physiology, 2015. **88**(3): p. 168-178.

19. Mattei, A.L., et al., *Integrated 3D view of postmating responses by the Drosophila melanogaster female reproductive tract, obtained by micro-computed tomography scanning.* Proceedings of the National Academy of Sciences, 2015. **112**(27): p. 8475-8480.

20. Lim, J., et al., *The Octopamine Receptor Octβ2R Regulates Ovulation in Drosophila melanogaster.* PLoS ONE, 2014. **9**(8): p. e104441-e104441.